

Series expansion studies of random sequential adsorption with diffusional relaxation

Chee Kwan Gan and Jian-Sheng Wang
*Department of Computational Science,
 National University of Singapore, Singapore 119260,
 Republic of Singapore.*
 (29 July, 1996)

We obtain long series (28 terms or more) for the coverage (occupation fraction) θ , in powers of time t for two models of random sequential adsorption with diffusional relaxation using an efficient algorithm developed by the authors. Three different kinds of analyses of the series are performed for a wide range of γ , the rate of diffusion of the adsorbed particles, to investigate the power law approach of θ at large times. We find that the primitive series expansions in time t for θ capture rich short and intermediate time kinetics of the systems very well. However, we see that the series are still not long enough to extract the kinetics at large times for general γ . We have performed extensive computer simulations employing an efficient event-driven algorithm to confirm the $t^{-1/2}$ saturation approach of θ at large times for both models, as well as to investigate the short and intermediate time behaviors of the systems.

PACS number(s): 05.70.Ln, 82.20.Mj, 75.40.Mg, 05.50.+q

INTRODUCTION

Random sequential adsorption (RSA) [1] is an irreversible process which particles are deposited randomly and consecutively on a surface. The depositing particles, represented by hard-core extended objects, satisfy the excluded volume condition where they are not allowed to overlap. The exclusion of certain regions for further deposition attempts due to the adsorbed particles leads to a dominant infinite-memory correlation effect where the system approaches partially covered, fully blocked stage at large times. However, this picture is altered when the diffusional relaxation is introduced [2–4]. Privman and Nielaba [2] have shown that the effect of added diffusional relaxation in the deposition of dimer on a 1D lattice substrate is to allow the full, saturation coverage via a $\sim t^{-1/2}$ power law at large times, preceded by a mean-field crossover regime with the intermediate $\sim t^{-1}$ behavior for fast diffusion.

Series expansion is one of the powerful analytical methods in the RSA studies [5–10]. Long series in powers of time t have been obtained, reminiscent of series expansions in equilibrium statistical mechanics, by using a computer [11]. Recently, the authors [10] have proposed an efficient algorithm for generating long series for the coverage θ in powers of time t based on the hierarchical rate equations.

The present work is to study the time-dependent quantity θ for one-dimensional models of RSA with diffusional relaxation, both analytically and numerically. It will be seen that even though relatively long series have been obtained, we are still unable to extract the kinetics of the systems at large times for general γ due to long, rich transient crossover regime that the series must describe. Extensive computer simulations are performed to confirm the $t^{-1/2}$ power law approach of θ , where we have employed an efficient event-driven algorithm. The remainder of this paper is organized as follows. Section I introduces two related models. Details of series expansion are explained in Section II. Analyses of the series can be found in Section III. Monte Carlo results are presented in Section IV and finally Section V contains the summary and conclusions.

I. THE MODELS

Two models have been studied in this work. We start with an initially empty, infinite linear lattice. Dimers are dropped randomly and sequentially at a rate of k per lattice site per unit time, onto the lattice. Hereafter we set k equal to unity without loss of generality. If the chosen two neighbor sites are unoccupied, the dimer is adsorbed on the lattice. If one of the chosen sites is occupied, the adsorption attempt is rejected. One of the simplest possibilities of diffusional relaxation in this dimer adsorption process is that the adsorbed dimer is permitted to hop either to left or right by one lattice constant at a diffusion rate γ from the original dimer position, provided that the diffusion attempt does not violate the excluded volume condition. This model has been initiated and studied by Privman and Nielaba [2]. We refer this model as the dimer RSA with dimer diffusion or diffusive dimer model.

A second possibility is that an adsorbed dimer is allowed to dissociate into two independent monomers; each monomer can diffuse to one of its nearest neighbor sites with a diffusion rate γ , provided that the diffusion attempt does not violate the excluded volume condition. This model bears a strong resemblance to the former model and

is exactly solvable when $\gamma = 1/2$ [12]. We refer this model as the dimer RSA with monomer diffusion or diffusive monomer model. Interestingly enough, the special case of the diffusive monomer problem with $\gamma = 1/2$ can be mapped to the diffusion-limited process

$$\mathcal{A} + \mathcal{A} \rightarrow \text{inert}, \quad (1)$$

which is known as one-species annihilation process [13]. This model has been solved exactly by a number of researchers [14–16]. We observe that when $\gamma = 1/2$, the effect of a dimer deposition attempt in the diffusive monomer model corresponds to two diffusion attempts of \mathcal{A} in an adjacent pair of \mathcal{A} of the $\mathcal{A} + \mathcal{A} \rightarrow \text{inert}$ process. The time-dependent quantity coverage $\theta(t)$ (fraction of occupied sites) for the diffusive monomer model with $\gamma = 1/2$ is given by

$$\theta(t) = 1 - \exp(-2t)I_0(2t), \quad (2)$$

where $I_n(z)$ is the modified Bessel function of integer order n .

II. SERIES EXPANSIONS

To illustrate how series expansions are performed, we note that the first few rate equations for the dimer and monomer diffusive models are

$$\frac{dP(\circ)}{dt} = -2P(\circ\circ), \quad (3)$$

$$\frac{dP(\circ\circ)}{dt} = -P(\circ\circ) - 2P(\circ\circ\circ) - 2\gamma P(\circ\circ\bullet\bullet) + 2\gamma P(\circ\bullet\bullet\circ), \quad (4)$$

$$\frac{dP(\circ\circ\circ)}{dt} = -2P(\circ\circ\circ) - 2P(\circ\circ\circ\circ) - 2\gamma P(\circ\circ\circ\bullet\bullet) + 2\gamma P(\circ\circ\bullet\bullet\circ), \quad (5)$$

...

and

$$\frac{dP(\circ)}{dt} = -2P(\circ\circ), \quad (6)$$

$$\frac{dP(\circ\circ)}{dt} = -P(\circ\circ) - 2P(\circ\circ\circ) - 2\gamma P(\circ\circ\bullet) + 2\gamma P(\circ\bullet\circ), \quad (7)$$

$$\frac{dP(\circ\circ\circ)}{dt} = -2P(\circ\circ\circ) - 2P(\circ\circ\circ\circ) - 2\gamma P(\circ\circ\circ\bullet) + 2\gamma P(\circ\circ\bullet\circ), \quad (8)$$

$$\begin{aligned} \frac{dP(\circ\circ\bullet)}{dt} = & -P(\circ\circ\bullet) + P(\circ\circ\circ\circ) - \gamma P(\circ\circ\bullet) + \gamma P(\circ\bullet\circ) - \\ & \gamma P(\circ\circ\bullet\circ) + \gamma P(\circ\circ\circ\bullet), \end{aligned} \quad (9)$$

...

respectively, where $P(C)$ denotes the probability of finding a configuration C of sites specified empty ‘ \circ ’ or filled ‘ \bullet ’. Unspecified sites can be occupied or empty. Here we have taken into account the symmetries of a configuration under all lattice group operations. For the one-dimensional configurations, we just need to consider the reflection operation only.

Let C_o denote a particular configuration of interest, and $P_{C_o} \equiv P(C_o)$ the associated configuration probability. P_{C_o} is expected to be a well behaved function of time t , so one can obtain the Taylor series expansion with the expansion point at $t = 0$, $P_{C_o}(t) = \sum_{n=0}^{\infty} P_{C_o}^{(n)} t^n / n!$, with the n th derivative of P_{C_o} given by

$$P_{C_o}^{(n)} = \left. \frac{d^n P_{C_o}(t)}{dt^n} \right|_{t=0}. \quad (10)$$

Let G_i denote the set of new configurations generated in the calculation of the i th derivative of P_{C_o} , and G_i^j the corresponding j th derivatives of the set of configurations. We observe that $G_0^{n-1}, G_1^{n-2}, \dots, G_{n-1}^0$ (determined at the $(n-1)$ th derivative), $G_0^{n-2}, G_1^{n-3}, \dots, G_{n-2}^0$ (determined at the $(n-2)$ th derivative), \dots, G_0^0 are predetermined before calculating the n th derivative of P_{C_o} . In the calculation of n th derivative of P_{C_o} , we determine systematically $G_0^n, G_1^{n-1}, \dots, G_{n-1}^1, G_n^0$, by recursive use of rate equations. This algorithm is efficient since each value in G_i^{n-i} ,

$0 \leq i \leq n$ and the rate equation for a configuration C is generated once only. However, this algorithm consumes the memory quickly as a result of storage of intermediate results.

The computation of the expansion coefficients makes use of the isomorphism between a lattice configuration and its binary representation if we map an occupied (empty) site to 1 (0). The data structures used to represent Eq. (3) and Eq. (4) are depicted in Fig. 1. A node for a configuration C is characterized by its four components; (i) the representation of C in the computer, (ii) a pointer to the derivatives of P_C , $P_C^{(n)}$ for $n = 1, 2, 3, \dots$, (iii) the highest order of derivative h of P_C obtained so far, and (iv) a pointer to a linked list of nodes of configurations ('children') which appear in the right hand side of the rate equation for P_C . The linked list contains the associated coefficients for each 'child'. The variable h is used so that we know the values of $P_C^{(n)}$ where $1 \leq n \leq h$ have already been calculated and can be retrieved when needed. All pointers to the configuration nodes generated during the enumeration process are stored in a hash table or a binary tree to allow efficient checking of the existence of any configuration. Use of the algorithm and data structures allows us to obtain coefficients up to t^{31} and t^{27} (presented in Appendix A) for $P(\circ, t)$ of the diffusive dimer and monomer models, respectively.

III. ANALYSES OF SERIES

Analytically, we are interested in confirming the power law approach of $t^{-1/2}$ of the coverage θ at large times for both diffusive dimer and monomer models through the unbiased and biased analyses of the series. The unbiased analysis does not fix the saturation coverage of the system, while the biased analysis assumes the saturation coverage to be the value 1. For the unbiased analysis, let $\theta(t) = 1 - P(\circ, t)$ be the time dependent coverage. Let assume that at very large times t the coverage θ satisfies the equation

$$\theta(t) = \theta_c - \frac{A(t)}{t^\delta}, \quad (11)$$

where θ_c is the saturation coverage. $A(t)$ is assumed to be a function of t , which tends to a constant value as $t \rightarrow \infty$, and δ is the exponent that characterizes the saturation approach (we expect to obtain $\delta = 1/2$ from the analysis of the series for all γ values). Writing $t = A(t)^{1/\delta}(\theta_c - \theta)^{-1/\delta}$, we see that if we perform a DLog Padé [17–19] analysis to the inverted series $t = t(\theta)$, where

$$\frac{d}{d\theta} \log t(\theta) = \frac{1}{\delta} \frac{d}{d\theta} \log A(t) - \frac{1}{\delta} \cdot \frac{1}{\theta - \theta_c}, \quad (12)$$

then the power law of Eq. (11) implies a simple, isolated pole of θ_c with an associated residue of $-1/\delta$. Fig. 2 shows the plot of the inverted series t versus θ for the 28-term series with $\gamma = 1/2$ for the monomer diffusive model.

For the diffusive dimer problem, the closest real pole to the value 1 (the expected saturation coverage) for [16,15], [15,16], [15,15], [16,14], and [14,16] Padé approximants are shown in Fig. 3, with the corresponding saturation exponents δ displayed in Fig. 4. Similarly we form [14,13], [13,14], [13,13], [14,12], [12,14] Padé approximants for the diffusive monomer problem, where the results are displayed in Fig. 5 and Fig. 6. Comparing the graphs for these two models, the diffusive dimer series give a better convergence of θ_c and δ against γ than that for the diffusive monomer series generally, presumably due to the fact that the coefficients of the series of $P(\circ, t)$ alternate in signs in the former model. For small γ values ($\gamma < 5$), the estimates for θ_c and δ are unstable — different Padé approximants do not agree with one another. The series with $\gamma = 0$ describes a pure lattice RSA behavior [6], where the system approaches the jamming coverage exponentially. Hence we expect the confirmation for power law of Eq. (11) is interfered by the exponential behavior of the series when γ is small. For $\gamma > 5$, there are physically favorable estimates for θ_c and δ where $\theta_c = 1.00 \pm 0.05$ and $\delta = 1.0 \pm 0.1$ for $10 < \gamma < 20$, for both models. These results are the manifestations of the transient regime of t^{-1} approach to saturation.

The distribution plot of the poles and zeros in the vicinity of (1,0) is displayed in Fig. 7 for the [14,13] Padé approximant for the 28-term series with $\gamma = 1/2$ for the diffusive monomer model. We see that the real pole closest to (1,0) is not distinguished and isolated from the nearby poles and zeros. This explains the difficulty of unbiased analysis that the intermediate crossover effect masks the power law approach at late stages.

We also perform biased analyses for the series. This series analysis have been used by Jensen and Dickman [23] to extract critical exponents from series in powers of time t . We define the F -transform of $f(t)$ by

$$F[f(t)] = t \frac{d}{dt} \ln f. \quad (13)$$

If $f \sim At^{-\alpha}$ for some constant A , then $F(t) \rightarrow \alpha$ as $t \rightarrow \infty$. We consider the exponential transformation

$$z = \frac{1 - e^{-bt}}{b}, \quad (14)$$

which proved to be very useful in the analysis of RSA series [6,10,23]. This transformation involves a parameter b which cannot be fixed a priori is then followed by the construction of various orders of Padé approximants to the z -series. Crossing region is then searched for in the graphs of α versus b , the transformation parameter.

To illustrate this biased analysis, we take the saturation coverage θ_c to be 1 and choose $f(t)$ to be $P(\circ, t) = \theta_c - \theta(t)$. Since we expect $P(\circ, t) \sim t^{-1/2}$ for large times t , specifically we have formed [14,13], [13,14], [13,13], [14,12], [12,14] Padé approximants to the z -series for the 28-term series with $\gamma = 1/2$ for the diffusive monomer model. We find that the estimates for δ is 0.5061(5), for $0.45 < b < 0.50$, as we can see from Fig. 8. Thus the exact analytical function of $\exp(-2t)I_0(2t)$ serves as a useful guide of this analysis, where the exponent deviates from the value $1/2$ by only about 1%.

Given a value of γ , we obtain the corresponding estimates of δ from the first convergence of all Padé approximants by locating the crossing region. The results of δ estimates for several values of γ are presented in Table I. The corresponding uncertainties for δ which reflect the variation of δ over a range of b are shown in the same table. For the diffusive dimer model, we have formed [16,15], [15,16], [15,15], [16,14], [14,16], [15,14], and [14,15] Padé approximants to the z -series. The corresponding graphs are displayed in Fig. 9. It is seen that for small values of γ , we obtain small estimates of δ , while for large γ , $\delta \rightarrow 1$, suggesting the approach to the limiting saturation is via a mean-field like result, i.e. the t^{-1} power law. Hence we see that even though the exponential transformation Eq. (14) works well for the exact series of diffusive monomer model when $\gamma = 1/2$, its use for general γ is not very appropriate. We have also tried the transformation $z = 1 - (1 + bt)^{-1/2}$ to the series for both diffusive models but the convergence is rather poor.

We have tried and used a third method of extracting the saturation exponent δ . If we assume that for large enough times t , the saturation coverage θ assumes a power law

$$1 - \theta \propto t^{-\delta}, \quad (15)$$

then we expect a plot of $d \ln(1 - \theta)/d \ln(t)$ versus t or $\log_{10}(t)$ should give a plateau of constant $-\delta$ values. By forming [14,13], [13,14], [13,13] Padé approximants to the $d \ln(1 - \theta)/d \ln(t)$ of the 28-term series for the diffusive monomer model with $\gamma = 1/2$, we observe from Fig. 10 that the agreement between different Padé estimates and the exact solution is excellent for $\log_{10}(t)$ up to around 0.9. For diffusive dimer problem, three Padé approximants of [16,15], [15,16], and [15,15] are formed. The plots of $d \ln(1 - \theta)/d \ln(t)$ versus $\log_{10}(t)$ for the diffusive dimer and monomer models, shown in Fig. 11 and Fig. 12, respectively, are obtained by taking the average of the 3 different Padé estimates. The graphs end before the difference between at least a pair of Padé estimates is more than 0.001. The last estimates in Fig. 11 and Fig. 12 are taken as the estimates for δ and they are listed in the last two columns of Table I. These estimates for δ are plotted in the same graph for the F -transformed analysis for comparisons (Fig. 9). It is seen that our last method of extracting the saturation exponents appears to be better than the F -transform analysis since it yields almost about the same estimates for δ . It does not involve any transformation which is not known in advance that will yield consistent results [23]. Looking at the ends of the curves in Fig. 11 and Fig. 12, we are certain that the power law regime is still not reached since the δ estimates do not seem to converge to a constant value, except the case when $\gamma = 1/2$ for the diffusive monomer model. From this we know that our estimates for δ do not describe the true power law approach at large times t . Such information cannot be found in the F -transform analysis. We note that our last method of analyzing the series is easy to use compared to the F -transform analysis.

IV. MONTE CARLO SIMULATIONS

To study the short and large time behaviors of the coverage, we have performed extensive and exhaustive simulations for the diffusive dimer and monomer models. For both models, we take an initially empty linear lattice with $N = 20000$ sites with periodic boundary conditions so that the finite-size effects can be ignored. In each Monte Carlo step, a pair of adjacent sites is chosen randomly. The type of attempted process is then decided: deposition with probability p , where $0 < p \leq 1$, or diffusion with probability $(1 - p)$. In the case of the deposition attempts, if any one of the chosen sites is occupied, the deposition attempt is rejected (unsuccessful attempt), else the adsorption attempt is accepted. In the case of diffusion, yet another decision is made either to move right or left, with equal probability. If the selected decision is diffusion to the right, we check the selected pair of sites are occupied and its right nearest neighbor site is unoccupied, then the dimer is moved by one lattice constant to the right. The left-diffusion attempts are treated similarly. In contrast to the diffusive dimer model, the diffusive monomer model allows monomers to move by one lattice constant.

We define one time unit interval ($\Delta t = 1$) to be during which a deposition attempt is performed for each lattice site. Thus for N -site lattice, one unit time corresponds to N deposition attempts, on average. The diffusion rate γ relative to the deposition rate, is then $\gamma = (1 - p)/2p$.

Straightforward simulation procedure, as described above, encounters a serious drawback in which at late stages, most adsorption and diffusion attempts are rejected. In order to study the behavior of the system at large times, we have used an event-driven algorithm to speed up the dynamics of the simulations [20,21]. Let q be the probability that we can make a successful move, then the probability that the first $(i-1)$ th trials is unsuccessful, and the i th trial is successful is

$$P_i = q(1-q)^{i-1}, \quad i = 1, 2, 3, \dots \quad (16)$$

If we restrict all trials to be coming from the successful ones, then two consecutive trials are in fact separated by a random variable i in Eq. (16). This distribution can be generated by

$$i = \left\lfloor \frac{\ln \xi}{\ln(1-q)} \right\rfloor + 1, \quad (17)$$

where ξ is a uniformly distributed random number between 0 and 1. In employing this method, we have to keep and update an active list of successful moves/attempts, where from its length we can evaluate q at any instance.

Simulations are performed on a cluster of fast workstations. Our numerical results are obtained for $\gamma = 0.05, 0.10, 0.20, \dots$, and 6.40, for t up to 2^{20} . Each data set is averaged over 500 runs, and the longest run take about 150 CPU hours on a HP712/60. The coverage (fraction of occupied sites), $\theta(t)$, is plotted in Fig. 13 and Fig. 14 for the diffusive dimer and monomer models, respectively. We have also performed the simulation at $\gamma = 1/2$ for the diffusive monomer model in order to compare the simulation results with the exact results. It is seen that the agreement between them are so good that actually an overlapping line is observed in Fig. 14. For $\gamma = 0$, we have the exact solution [6]

$$\theta(t) = \frac{1 - \exp(-2(1 - \exp(-t)))}{2}. \quad (18)$$

For extremely fast diffusion case, i.e., $\gamma = \infty$, exact results have been obtained, where

$$t(\theta) = \frac{1}{4} \left(\frac{1}{1-\theta} - 1 \right) - \frac{1}{4} \ln(1-\theta), \quad (19)$$

for the diffusive dimer model [22] and

$$t(\theta) = \frac{1}{2} \left(\frac{1}{1-\theta} - 1 \right). \quad (20)$$

for diffusive monomer model. The approach of $(\theta_c - \theta) \sim t^{-1}$ at all times is obvious for these extremely fast diffusion models. We have included the lines of slope $-1/2$ to indicate the $t^{-1/2}$ power law clearly. It is seen from Fig. 13 and Fig. 14 that for $\gamma \geq 3.20$, the system takes a very long time ($t \approx 10^4$) before it can enter the final $t^{-1/2}$ regime. This explain why we have difficulty in extracting the actual power law approach from the primitive expansion in time t .

To further confirm that the saturation approach indeed follows a power law, we have used a scaling analysis. For large times t , let us assume that $(1-\theta)$ has the following scaling form

$$1 - \theta = (\gamma t)^{-1/2} G(\gamma^b/t), \quad (21)$$

where G is a scaling function and b is a constant to be determined. Eq. (21) requires that $G(u)$ tends to a constant when u tends to 0 [24]. This is required because for large times t , $(1-\theta) \sim t^{-1/2}$. Let further assume that for large u , $G(u) \sim u^z$ for some constant z . For extremely large γ , we have $(1-\theta) \sim t^{-1}$ (see Eqs. (19) and (20)) hence $z = 1/2$ and $b = 1$. Writing Eq. (21) as

$$\begin{aligned} 1 - \theta &= (1/\gamma)(\gamma/t)^{1/2} G(\gamma/t) \\ &\equiv (1/\gamma) F(t/\gamma), \end{aligned}$$

we then make log-log plots of $\gamma(1-\theta)$ versus t/γ for the diffusive dimer and monomer models as shown in Figs. 15 and 16, respectively. It is seen that the data collapse into single curves at large times t . Our numerical data confirm not only the power law decay but also a scaling behavior for $(1-\theta)$.

V. CONCLUSIONS

By using an efficient algorithm based on the hierarchical rate equations, relatively long series are obtained for two models of 1-d RSA with diffusional relaxation. Analyses of series are performed, but it is seen that even though the series are long, we only manage to extract the behaviors of the systems up to intermediate times only. To study the power law of a system at large times t , we see that a series which exhibits a continuous crossover behavior in its short and intermediate times ought to be long enough so that various orders of Padé approximants can still converge in the power law regime. Using these long series, we find that the analysis of series based on the ratio method by Song and Poland [25] was not useful. Specifically, for the diffusive monomer series when $\gamma = 1/2$ (which corresponds to the $A + A \rightarrow 0$ process in Song and Poland's work), we obtain the saturation exponent (where they have used the symbol ν) $\delta = 2.0, 1.2, 0.895, 0.729, 0.624, 0.551, 0.498, 0.458, 0.426, 0.401, 0.380, 0.363, 0.351, \dots$, which is not seen to be converging towards the expected value of $1/2$.

We have also performed extensive computer simulations using an efficient event-driven algorithm, where it allows us to use and simulate a larger system to much larger times t than it was done previously on a supercomputer [2]. The $t^{-1/2}$ power law approach of θ to its saturation is confirmed numerically at large times t .

ACKNOWLEDGEMENT

This work was supported in part by an Academic Research Grant RP950601 of National University of Singapore. Part of the calculations were performed on the facilities of the Computation Center of the Institute of Physical and Chemical Research, Japan. We would like to thank V. Privman for pointing out Ref. [12] and useful discussion on how to analyse the series. We also appreciate one of the referees for suggesting us to make a scaling behavior study.

-
- [1] J. W. Evans, Rev. Mod. Phys. **65**, 1281 (1993).
- [2] V. Privman and P. Nielaba, Europhys. Lett. **18**, 673 (1992).
- [3] P. Nielaba and V. Privman, Mod. Phys. Lett. B **6**, 533 (1992).
- [4] J. -S. Wang, P. Nielaba, and V. Privman, Mod. Phys. Lett. B **7**, 189 (1993).
- [5] A. Baram and D. Kutasov, J. Phys. A: Math. Gen. **22**, L251 (1989).
- [6] R. Dickman, J. -S. Wang, and I. Jensen, J. Chem. Phys. **94**, 8252 (1991).
- [7] M. J. de Oliveira and T. Tomé, Phys. Rev. A **46**, 6294 (1992).
- [8] B. Bonnier, M. Hontebeyrie and C. Meyers, Physica A **198**, 1 (1993).
- [9] A. Baram and M. Fixman, J. Chem. Phys. **103**, 1929 (1995).
- [10] C. K. Gan and J. -S. Wang, J. Phys. A: Math. Gen **29**, L177 (1996).
- [11] J. L. Martin, in *Phase Transitions and Critical Phenomena* **3**, ed. by C. Domb and M. S. Green (New York: Academic) p. 97.
- [12] M. D. Grynberg and R. B. Stinchcombe, Phys. Rev. Lett. **74**, 1242 (1995).
- [13] D. b. -Avraham, M. A. Burschka, and C. R. Doering, J. Stat. Phys. **60**, 695 (1990).
- [14] A. A. Lushnikov, Phys. Lett. A **120**, 135 (1987).
- [15] J. L. Spouge, Phys. Rev. Lett. **60**, 871 (1988).
- [16] D. Balding, P. Clifford, and N. J. B. Green, Phys. Lett. A **126**, 481 (1988).
- [17] G. A. Baker, Jr., Phys. Rev. **124**, 768 (1961).
- [18] D. L. Hunter and G. A. Baker, Jr., Phys. Rev. B **7**, 3346 (1973).
- [19] G. A. Baker, Jr. and D. L. Hunter, Phys. Rev. B **7**, 3377 (1973).
- [20] B. J. Brosilow, R. M. Ziff, and R. D. Vigil, Phys. Rev. A, **43**, 631 (1991).
- [21] J. -S. Wang, Inter. J. Mod. Phys. C **5**, 707 (1994).
- [22] V. Privman and M. Barma, J. Chem. Phys. **97**, 6714 (1992).
- [23] I. Jensen and R. Dickman, J. Stat. Phys. **71**, 89 (1993).
- [24] V. Privman (private communication).
- [25] S. Song and D. Poland, J. Phys. A **25**, 3913 (1992).

FIG. 1. The data structures used to represent the rate equations Eq. (3) and Eq. (4). The first field of the node associated with 'o' is the representation of the pattern 'o'. The second field points to its first four derivatives (i.e. -2, 6, -22, 94). The third field is the highest derivative, h obtained so far for $P(o)$; in this case h is 4. The rate equation is represented in the fourth field. The rate equation for the configuration 'oo' involves four configurations, one of them is 'oo' itself.

FIG. 2. The plot of the inverted series of time t versus coverage θ for the 28-term series with $\gamma = 1/2$ for the diffusive monomer model.

FIG. 3. The results for the saturation coverage θ_c as a function of the rate of diffusion γ obtained from the DLog Padé analysis of the inverted series of $t = t(\theta)$ with [16,15], [15,16], [15,15], [16,14], [14,16] Padé approximants for the diffusive dimer model. The saturation coverage estimates are very close to 1.

FIG. 4. The results for the saturation exponent, δ as a function of γ obtained from DLog Padé analysis of the inverted series $t = t(\theta)$ for the diffusive dimer model. These estimates for δ are deduced from the residues associated with the poles in Fig. 3.

FIG. 5. The results for the saturation coverage θ_c as a function of the rate of diffusion γ obtained from the DLog Padé analysis of the inverted series of $t = t(\theta)$ with [14,13], [13,14], [13,13], [14,12], [12,14] Padé approximants for the diffusive monomer model.

FIG. 6. The results for the saturation exponent, δ as a function of γ obtained from DLog Padé analysis of the inverted series $t = t(\theta)$ for the diffusive monomer model. These estimates for δ are deduced from the residues associated with the poles in Fig. 5.

FIG. 7. The distribution of zeros and poles in the vicinity of (1, 0) for the [14, 13] Padé approximant for the 28-term series with $\gamma = 1/2$ for the diffusive monomer model. A circle (cross) denotes a pole (zero).

FIG. 8. Padé approximant estimates for the exponent δ , as a function the transformation parameter b , derived from the F -transform analysis of the 28-term series with $\gamma = 1/2$ for the monomer diffusive model.

FIG. 9. The plot of the values in Table I. The diamonds and the squares denote the estimates of δ from the F -transform analysis for the diffusive dimer and monomer models, respectively. The crosses and the circles correspond to the estimates of δ from the $d \ln(1 - \theta)/d \ln(t)$ versus $\log_{10}(t)$ type analysis, for the diffusive dimer and monomer models, respectively. The error bars are smaller than the symbols and hence they are not displayed.

FIG. 10. The analysis based on the $d \ln(1 - \theta)/d \ln(t)$ versus $\log_{10}(t)$ plot for [14,13], [13,14], and [13,13] Padé approximants. We see that the agreement between three Padé estimates and the exact results is excellent for $\log_{10}(t)$ up to around 0.9.

FIG. 11. The plot of $d \ln(1 - \theta)/d \ln(t)$ versus $\log_{10}(t)$ for the diffusive dimer problem. All curves end before the difference between at least a pair of estimates from [16,15], [15,16], [15,15] Padé approximants is greater than 0.001. The ends of curves for $\gamma = 0.1, 0.2, \dots, 1.0, 1.5, 2.0, \dots, 5.0$, are displayed in the downward direction.

FIG. 12. The plot of $d \ln(1 - \theta)/d \ln(t)$ versus $\log_{10}(t)$ for the diffusive monomer problem. All curves end before the difference between at least a pair of estimates from [14,13], [13,14], [13,13] Padé approximants is greater than 0.001. The ends of curves for $\gamma = 0.1, 0.2, \dots, 1.0, 1.5, 2.0, \dots, 5.0$, are displayed in the downward direction.

FIG. 13. Monte Carlo simulation results for the diffusive dimer model. The sequence of γ for curves between the exact curves for $\gamma = 0$ and $\gamma = \infty$, in the downward direction, is 0.05, 0.10, 0.20, \dots , 6.40. The line of slope $-1/2$ shows the $t^{-1/2}$ approach at large times t .

FIG. 14. Monte Carlo simulation results for the diffusive monomer model. The sequence of γ for curves between the exact curves for $\gamma = 0$ and $\gamma = \infty$, in the downward direction, is 0.05, 0.10, 0.20, 0.40, 0.50, 0.80, 1.60, 3.20 and 6.40. Notice that the simulation results for $\gamma = 1/2$ and the exact results agree with each other extremely well that only one line is seen. The line of slope $-1/2$ shows the $t^{-1/2}$ approach at large times t .

FIG. 15. The scaling plot for the diffusive dimer problem. The sequence of γ , in the downward direction, is 6.40, 3.20, 1.60, ..., 0.05. The line of slope $-1/2$ is included to indicate the power law clearly.

FIG. 16. The scaling plot for the diffusive monomer problem. The sequence of γ , in the downward direction, is 6.40, 3.20, 1.60, ..., 0.05. The line of slope $-1/2$ is included to indicate the power law clearly.

TABLE I. The F -transform analysis gives the second and fourth columns which show the estimates of δ deduced from the crossing regions of the graphs of δ versus the transformation parameter b , taken in the range indicated in the third and fifth columns. The last two columns show the results obtained from the $d\ln(1-\theta)/d\ln(t)$ versus $\log_{10}(t)$ type analysis.

TABLE 1.

γ	dimer		monomer		dimer	monomer
	δ	b	δ	b		
0.1	0.431(3)	0.28 – 0.33	0.269(4)	0.65 – 0.70	0.407(1)	0.256(1)
0.2	0.499(2)	0.30 – 0.35	0.395(4)	0.30 – 0.35	0.510(1)	0.375(1)
0.3	0.542(2)	0.35 – 0.40	0.441(2)	0.35 – 0.40	0.566(1)	0.437(1)
0.4	0.573(3)	0.35 – 0.40	0.47788(4)	0.45 – 0.50	0.603(1)	0.479(1)
0.5	0.599(4)	0.36 – 0.41	0.5061(5)	0.45 – 0.50	0.618(1)	0.508(1)
0.6	0.623(5)	0.38 – 0.43	0.535(1)	0.75 – 0.80	0.662(1)	0.539(1)
0.7	0.649(4)	0.44 – 0.49	0.557(2)	0.85 – 0.90	0.682(1)	0.562(1)
0.8	0.669(5)	0.47 – 0.52	0.576(1)	0.90 – 0.95	0.716(1)	0.580(1)
0.9	0.685(5)	0.48 – 0.53	0.5915(6)	0.95 – 1.00	0.673(1)	0.595(1)
1.0	0.702(5)	0.51 – 0.56	0.6050(6)	1.00 – 1.05	0.684(1)	0.608(1)
1.5	0.759(5)	0.57 – 0.62	0.6534(3)	1.25 – 1.30	0.810(1)	0.650(1)
2.0	0.792(5)	0.58 – 0.63	0.6822(4)	0.95 – 1.00	0.830(1)	0.671(1)
2.5	0.830(3)	0.73 – 0.78	0.7041(4)	0.75 – 0.80	0.836(1)	0.693(1)
3.0	0.854(4)	0.80 – 0.85	0.718(2)	0.80 – 0.85	0.859(1)	0.708(1)
3.5	0.87(1)	0.81 – 0.86	0.730(3)	0.80 – 0.85	0.865(1)	0.704(1)
4.0	0.885(5)	0.88 – 0.93	0.742(4)	0.75 – 0.80	0.875(1)	0.705(1)
4.5	0.898(4)	0.90 – 0.95	0.746(4)	0.85 – 0.90	0.884(1)	0.710(1)
5.0	0.907(3)	0.95 – 1.00	0.752(4)	0.85 – 0.90	0.906(1)	0.707(1)

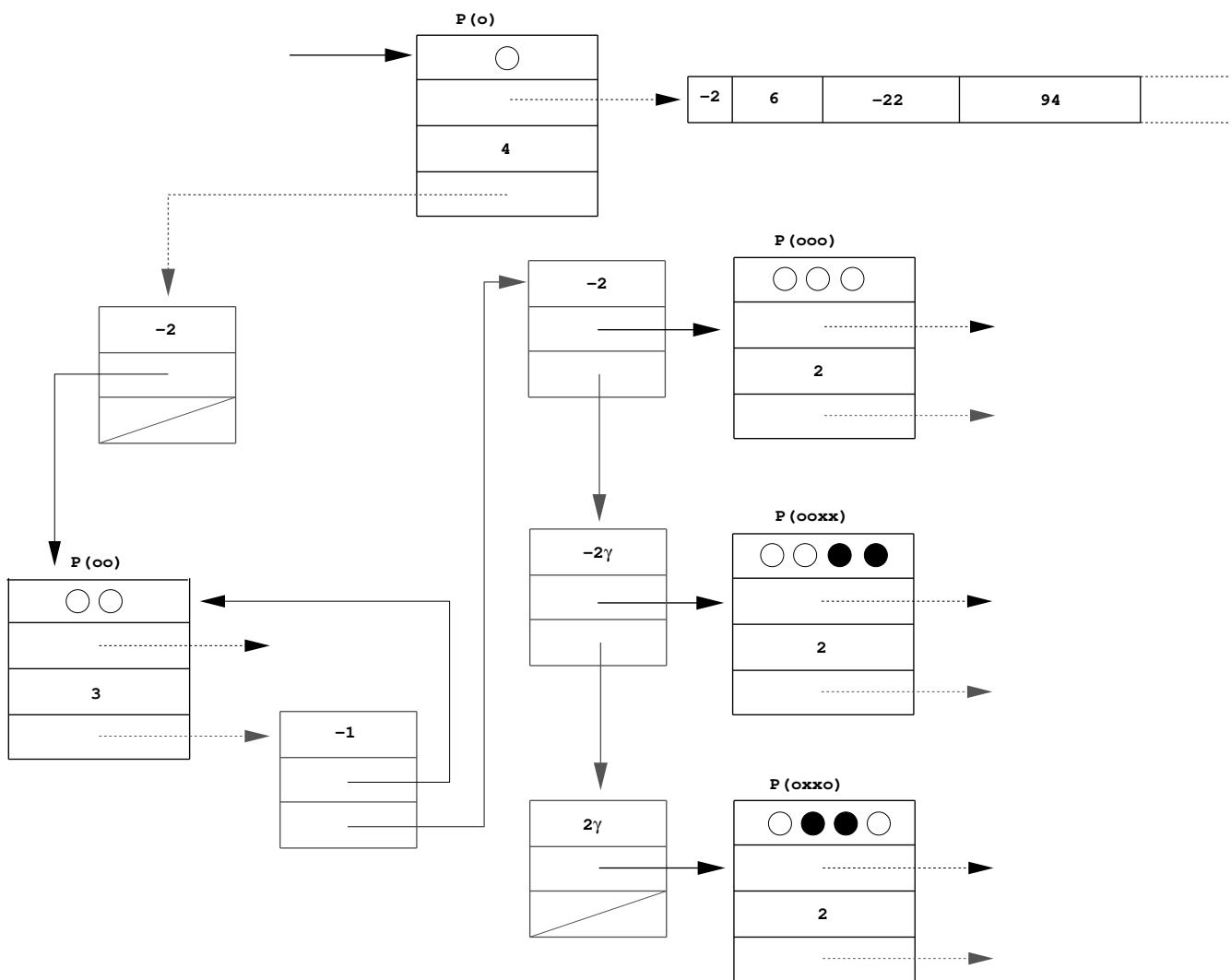


FIG.1.

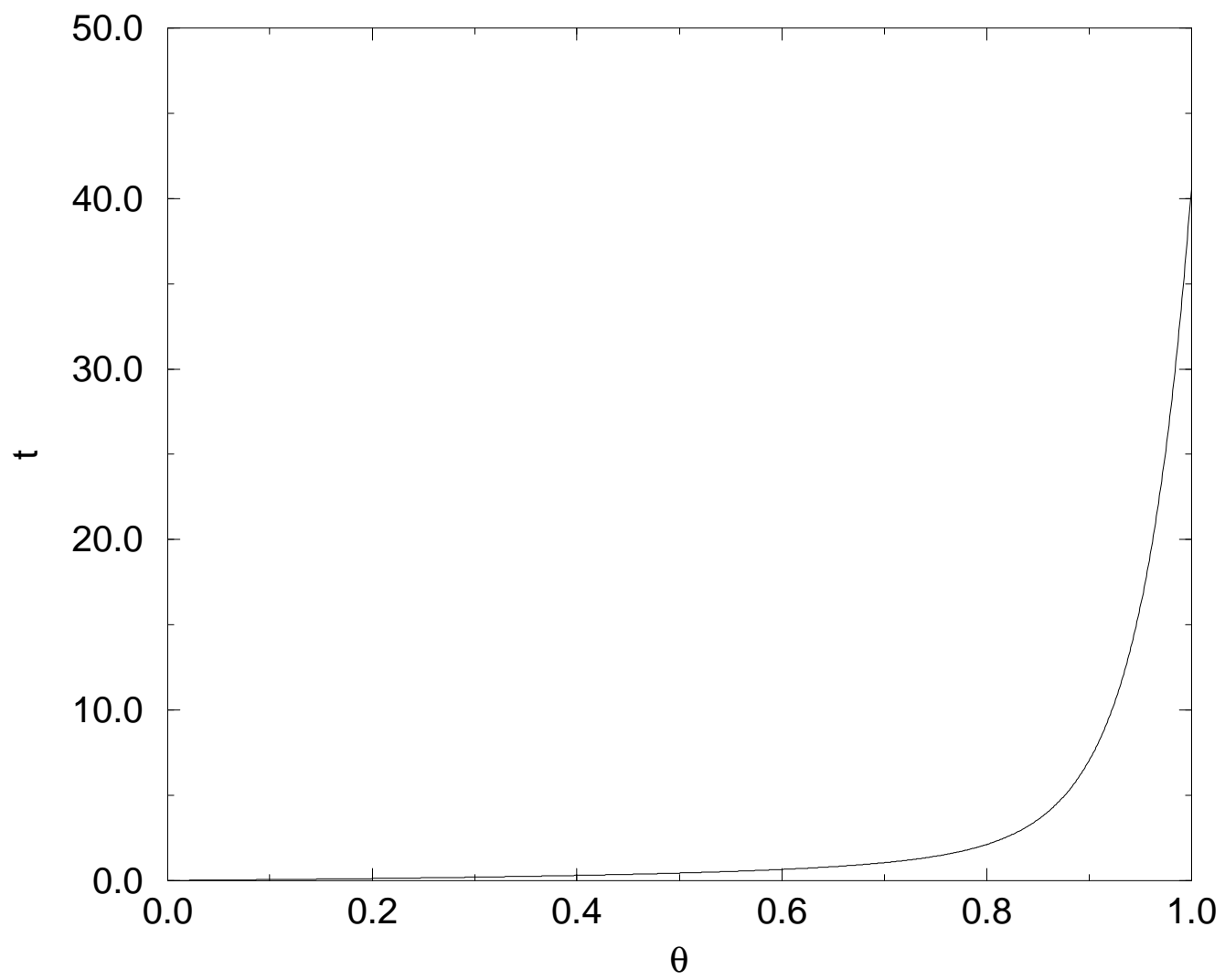


FIG.2.

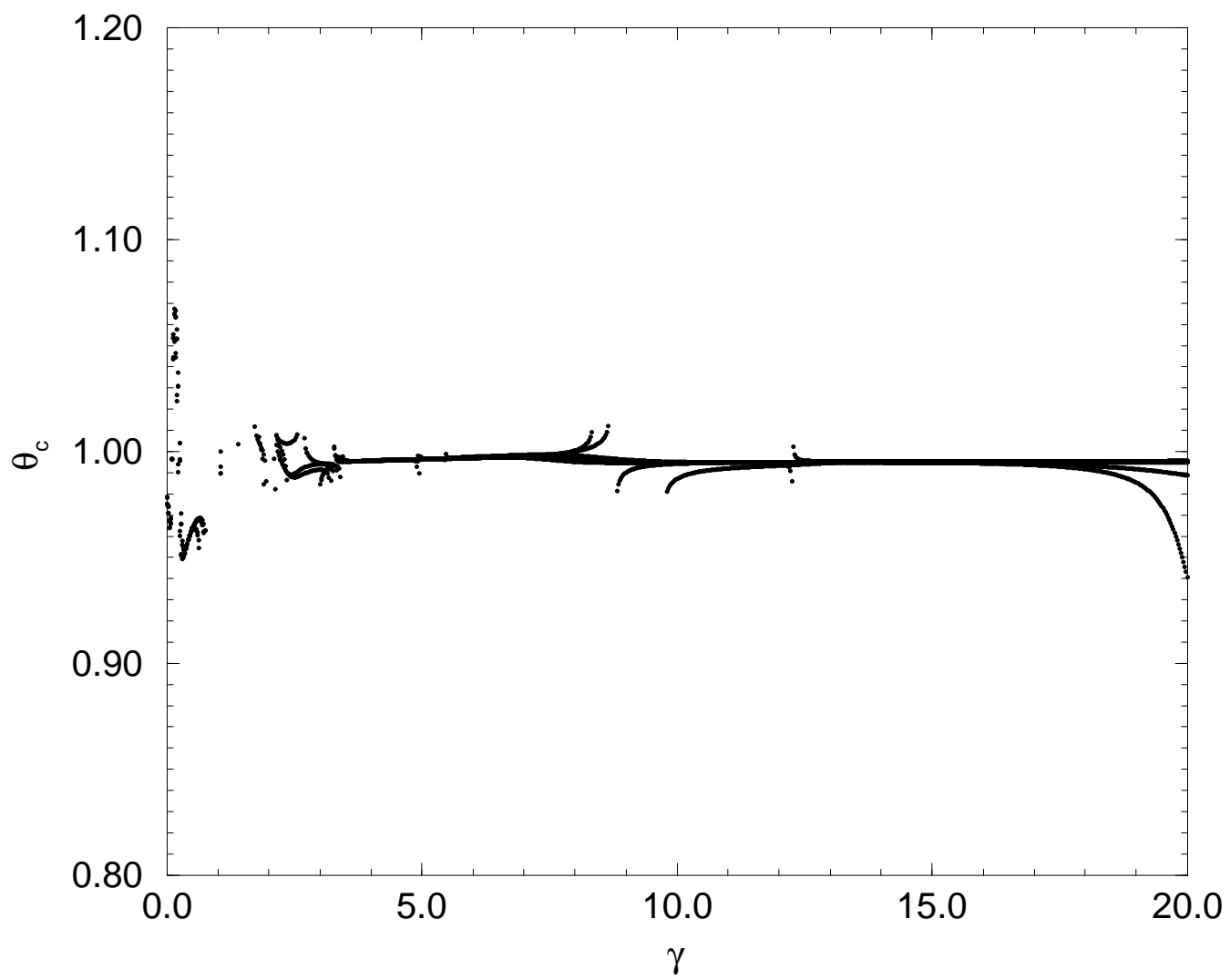


FIG.3.

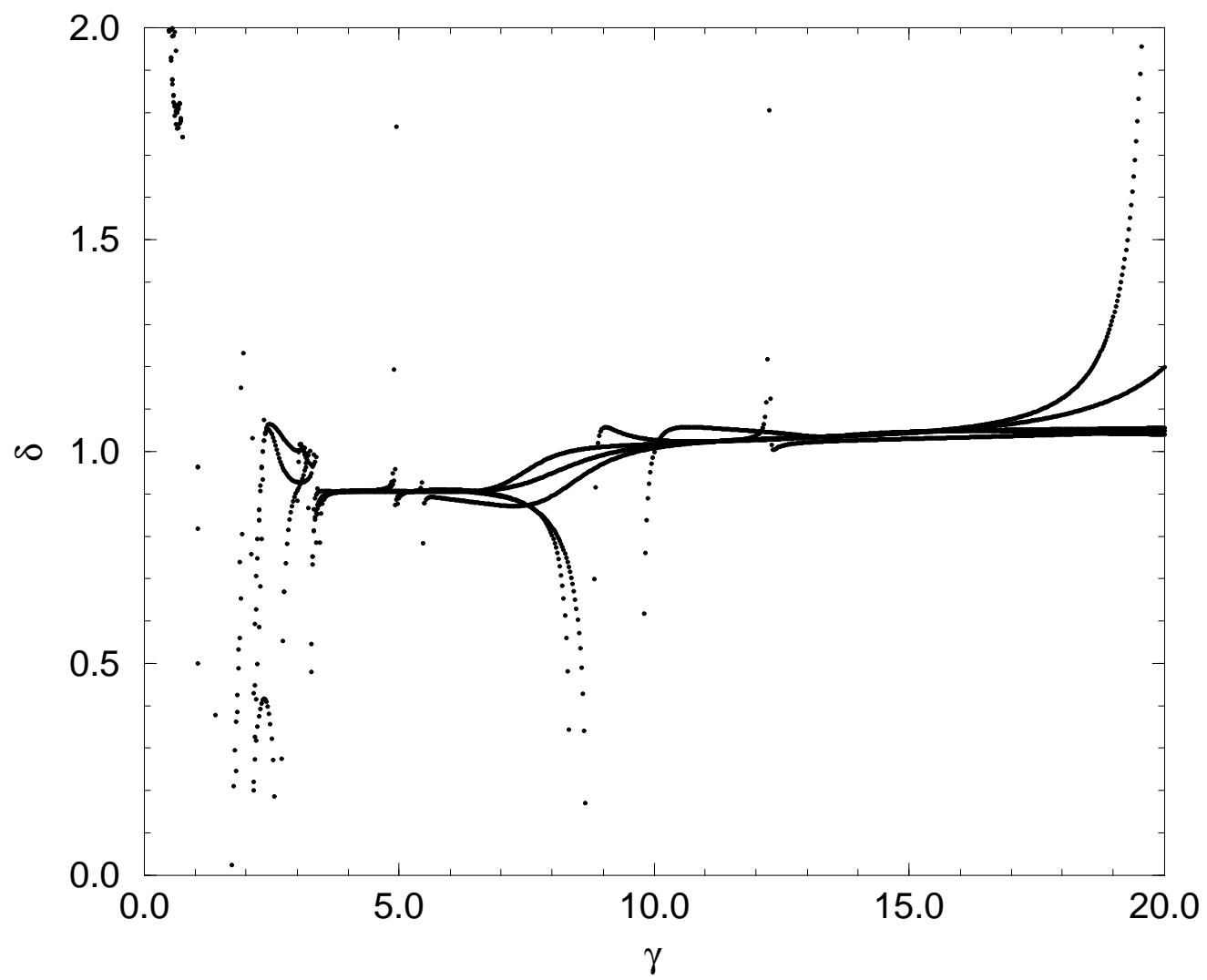


FIG.4.

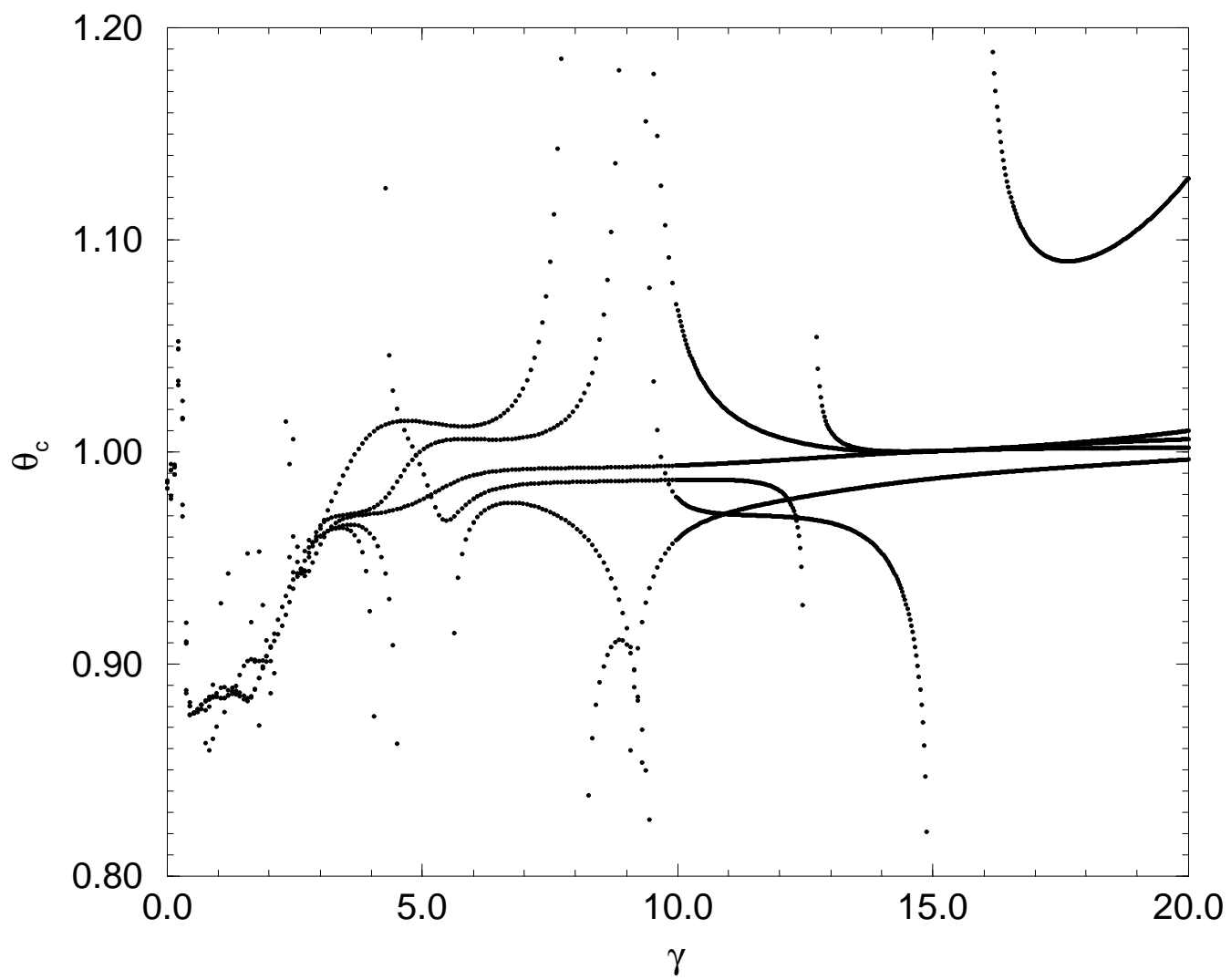


FIG.5.

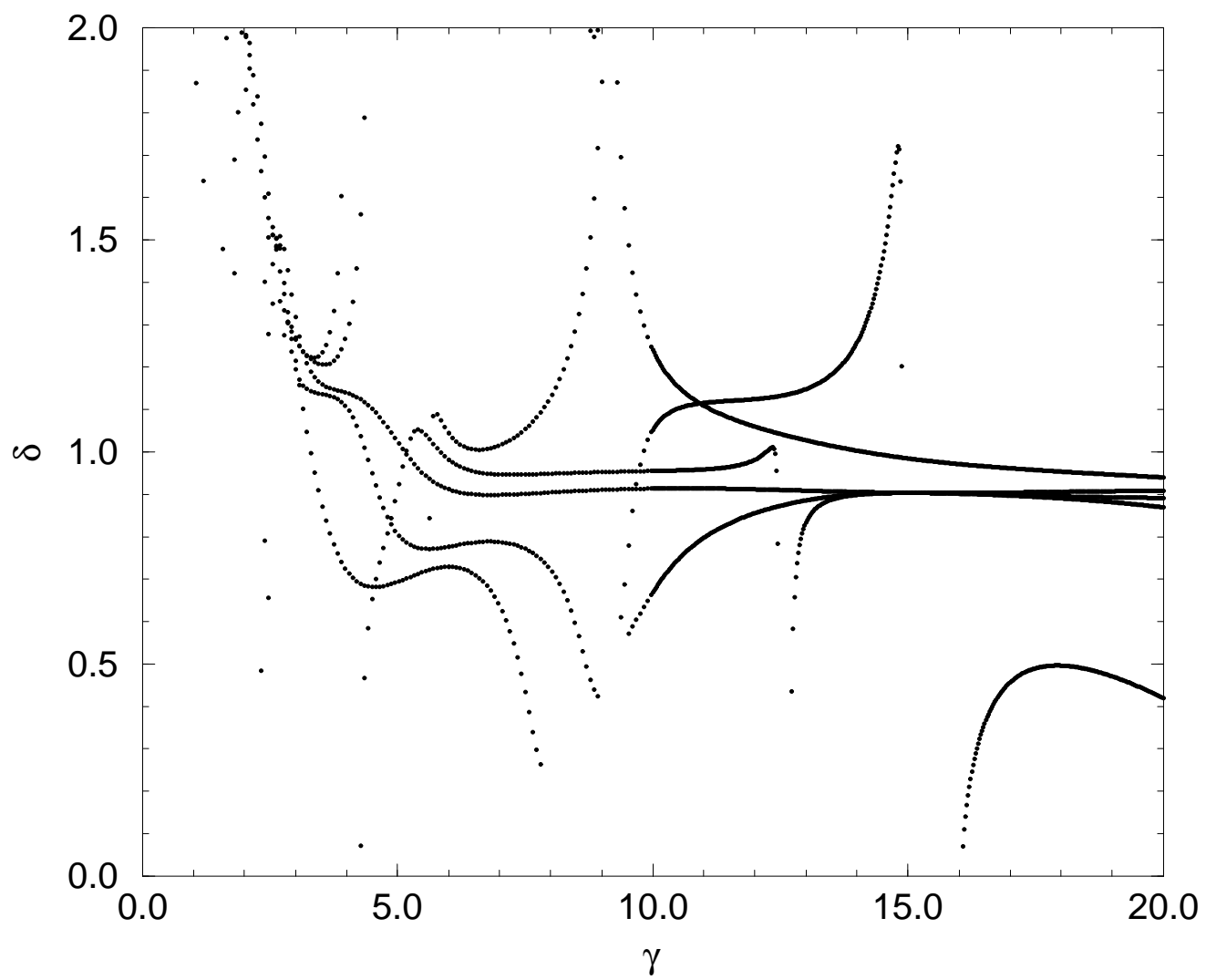


FIG.6.

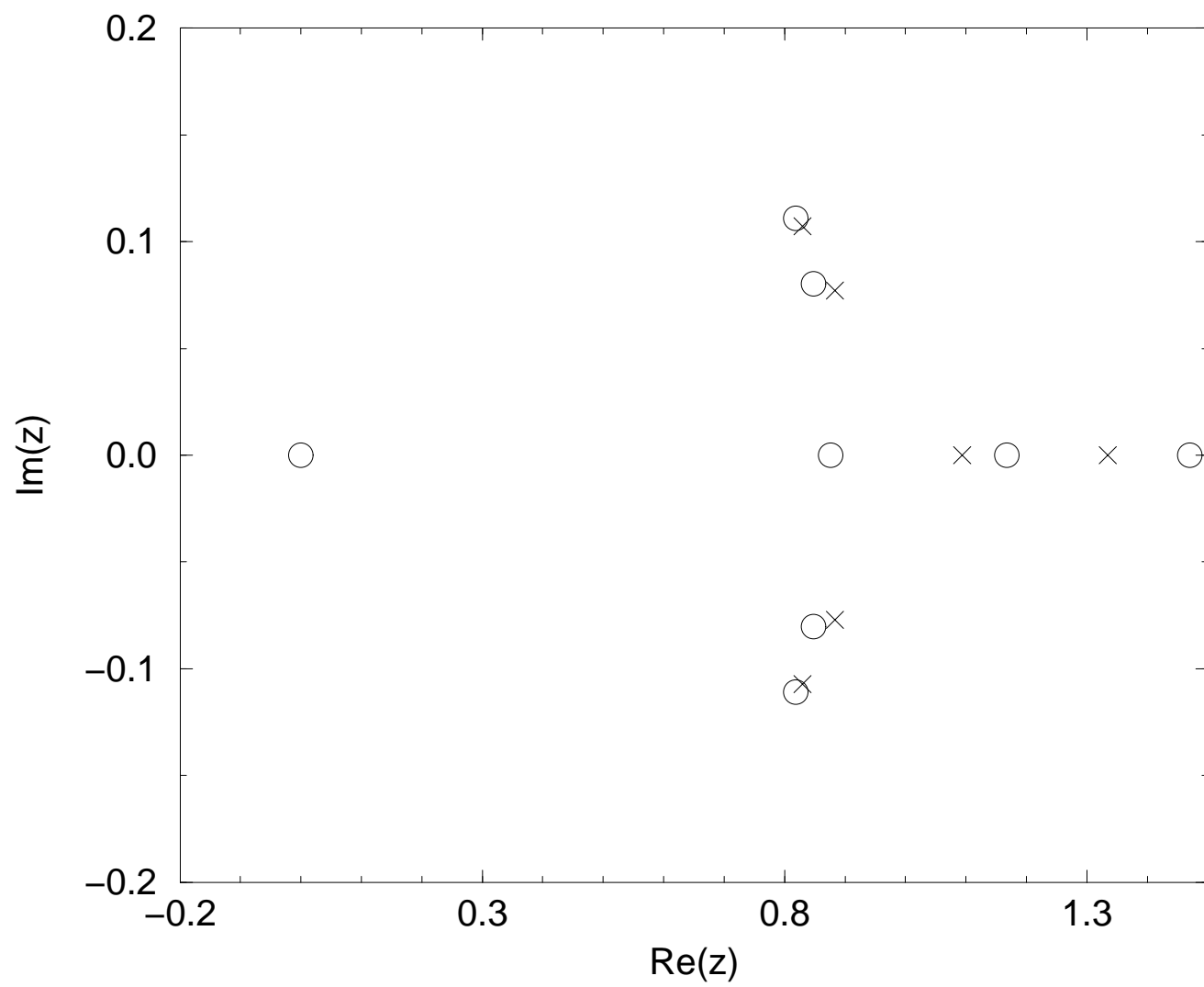


FIG. 7.

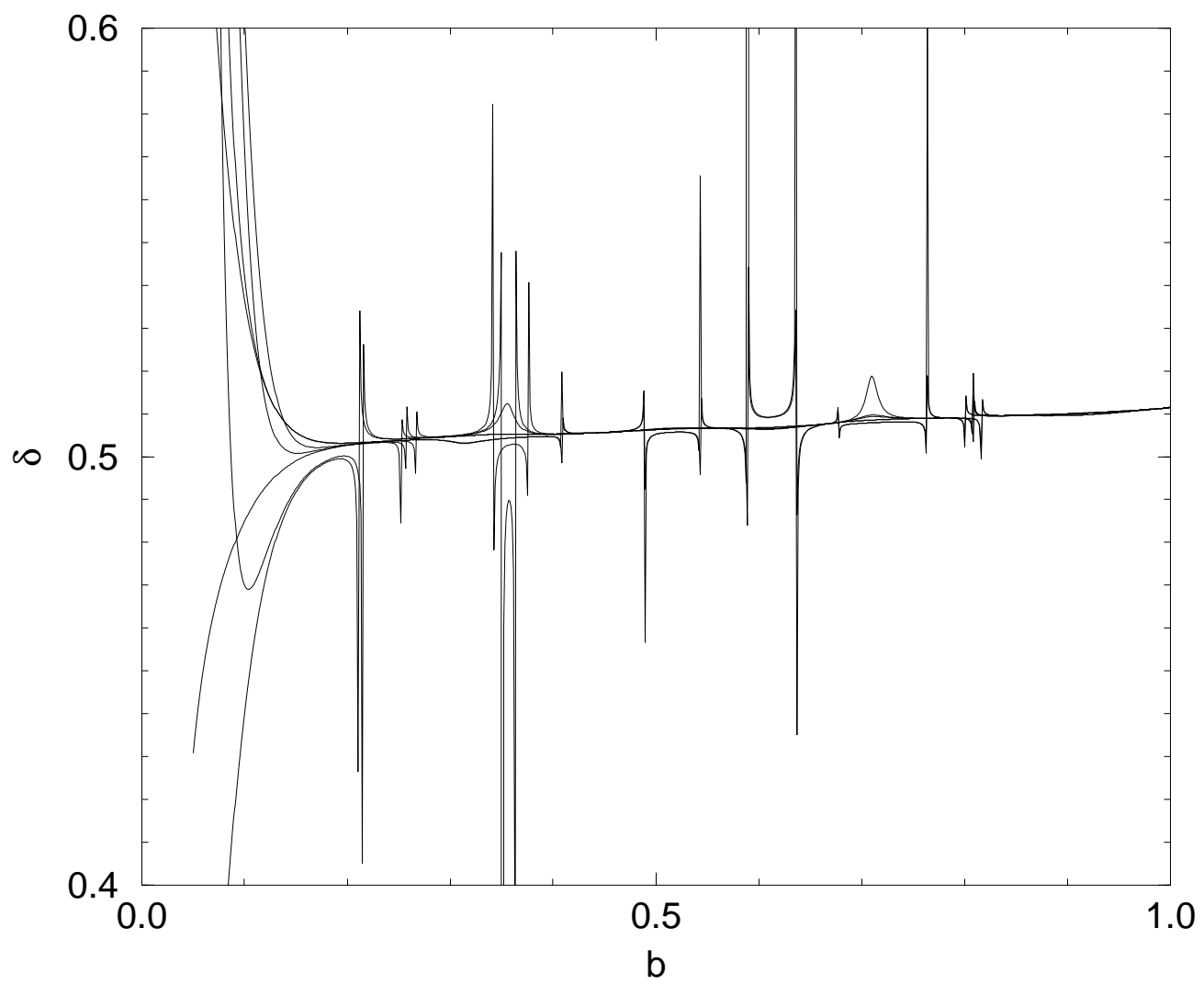


FIG.8.

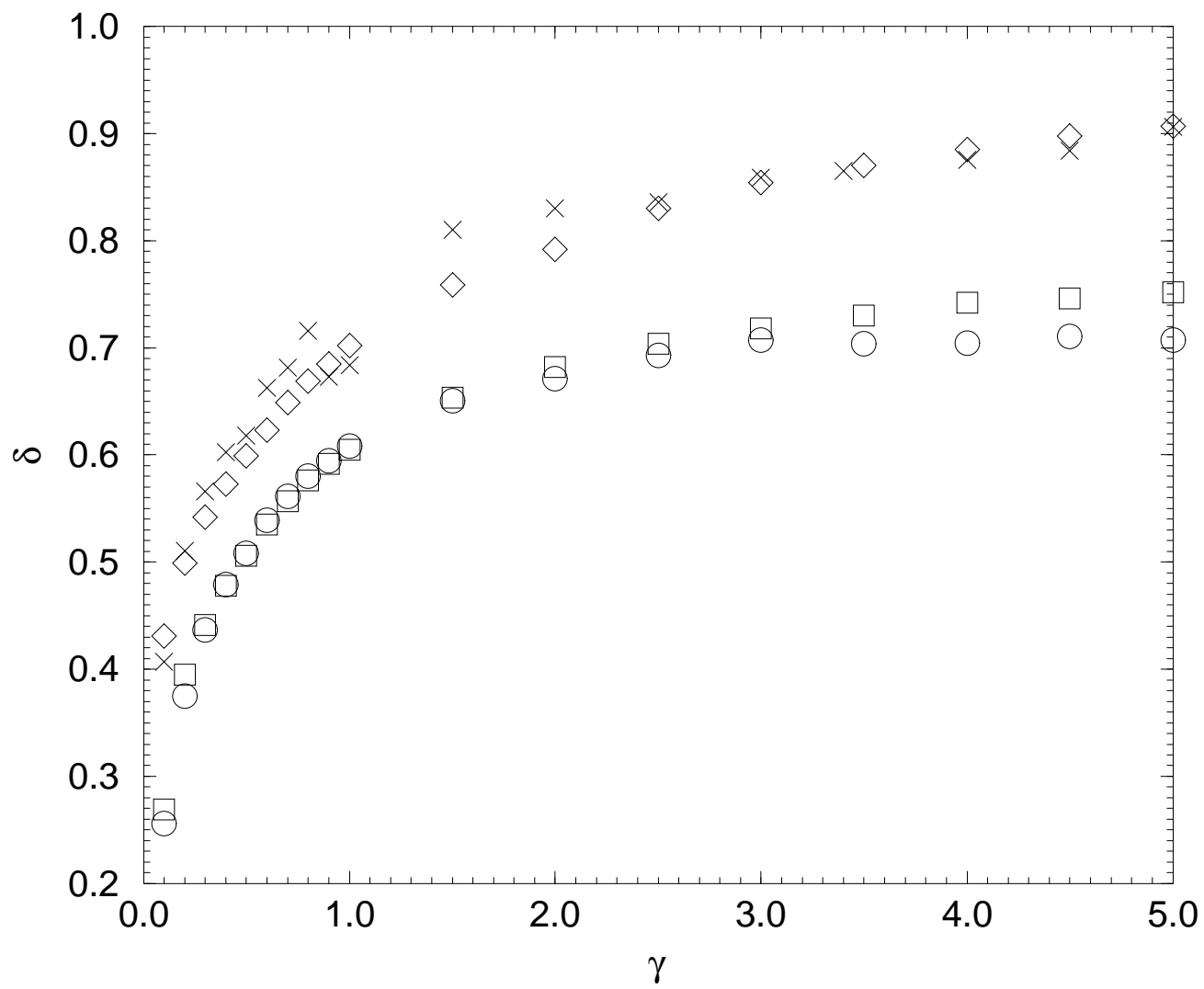


FIG.9.

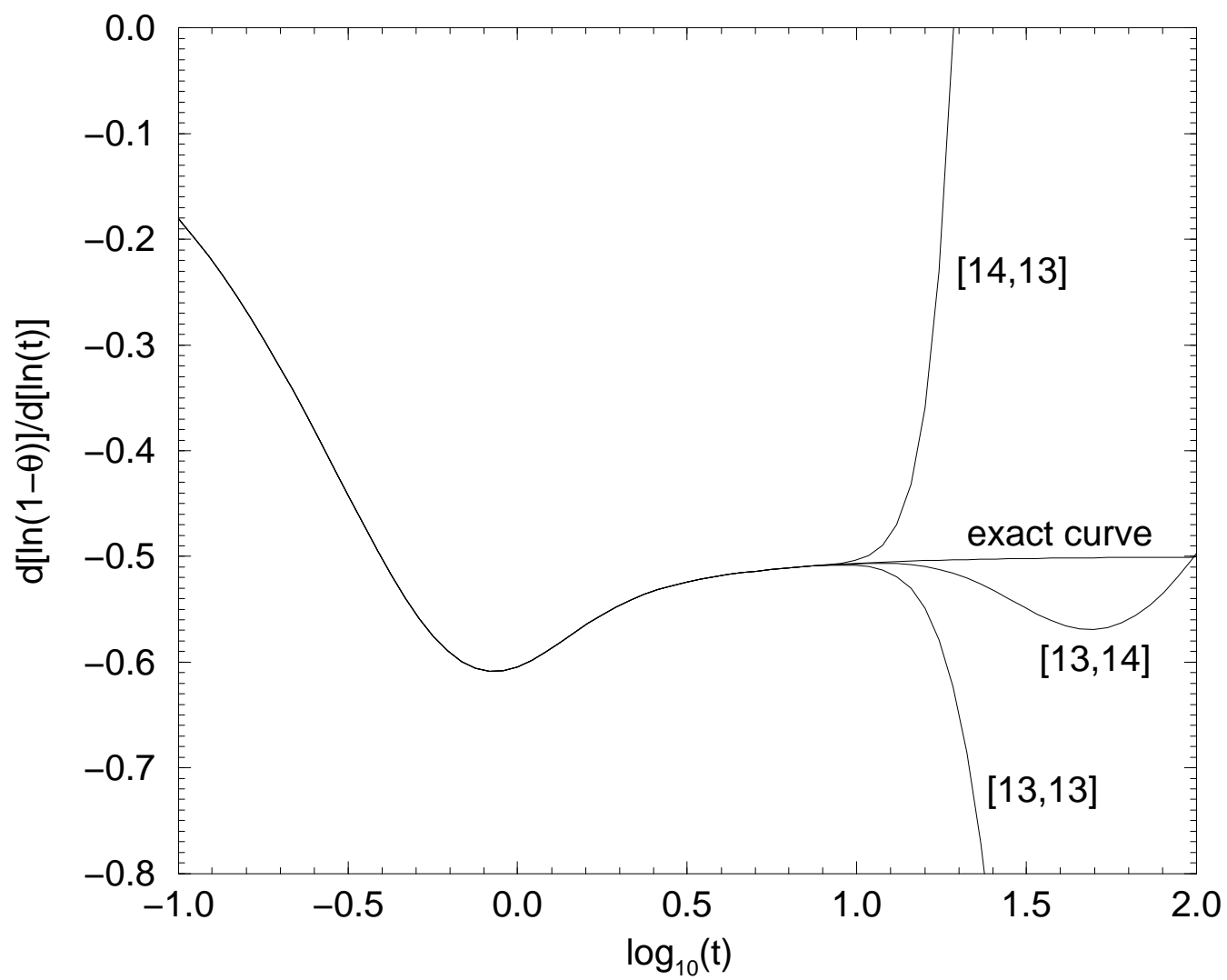


FIG.10.

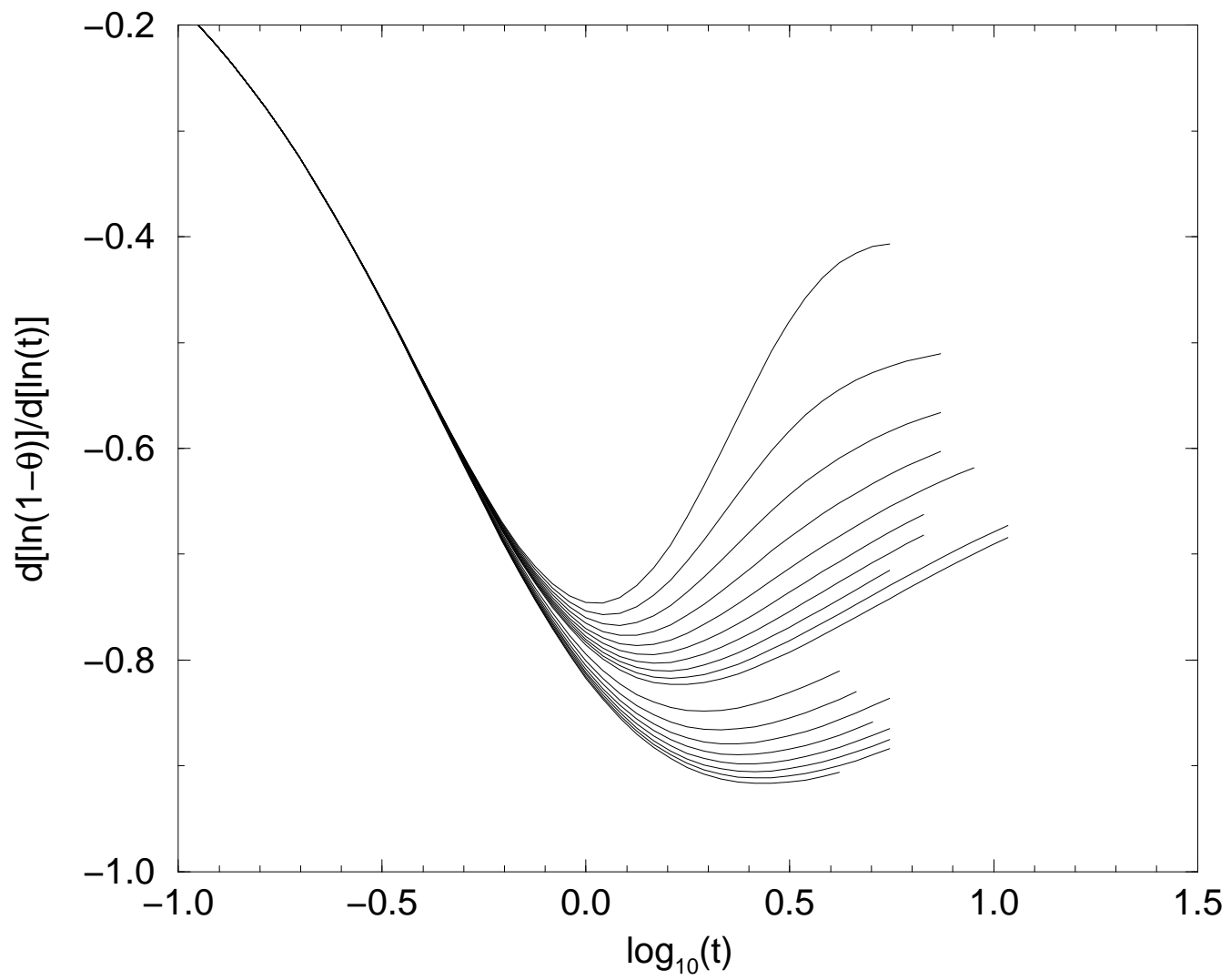


FIG.11.

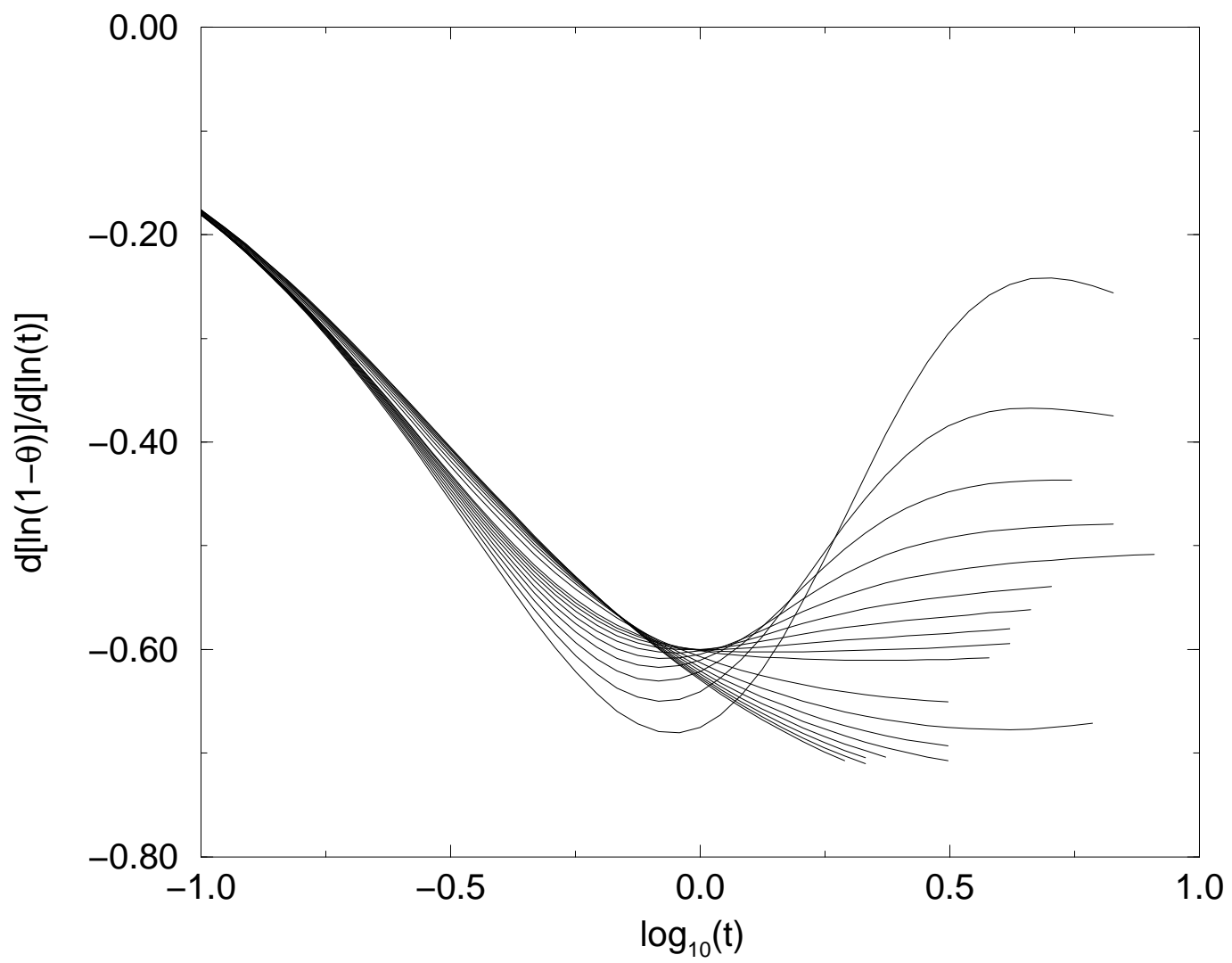


FIG.12.

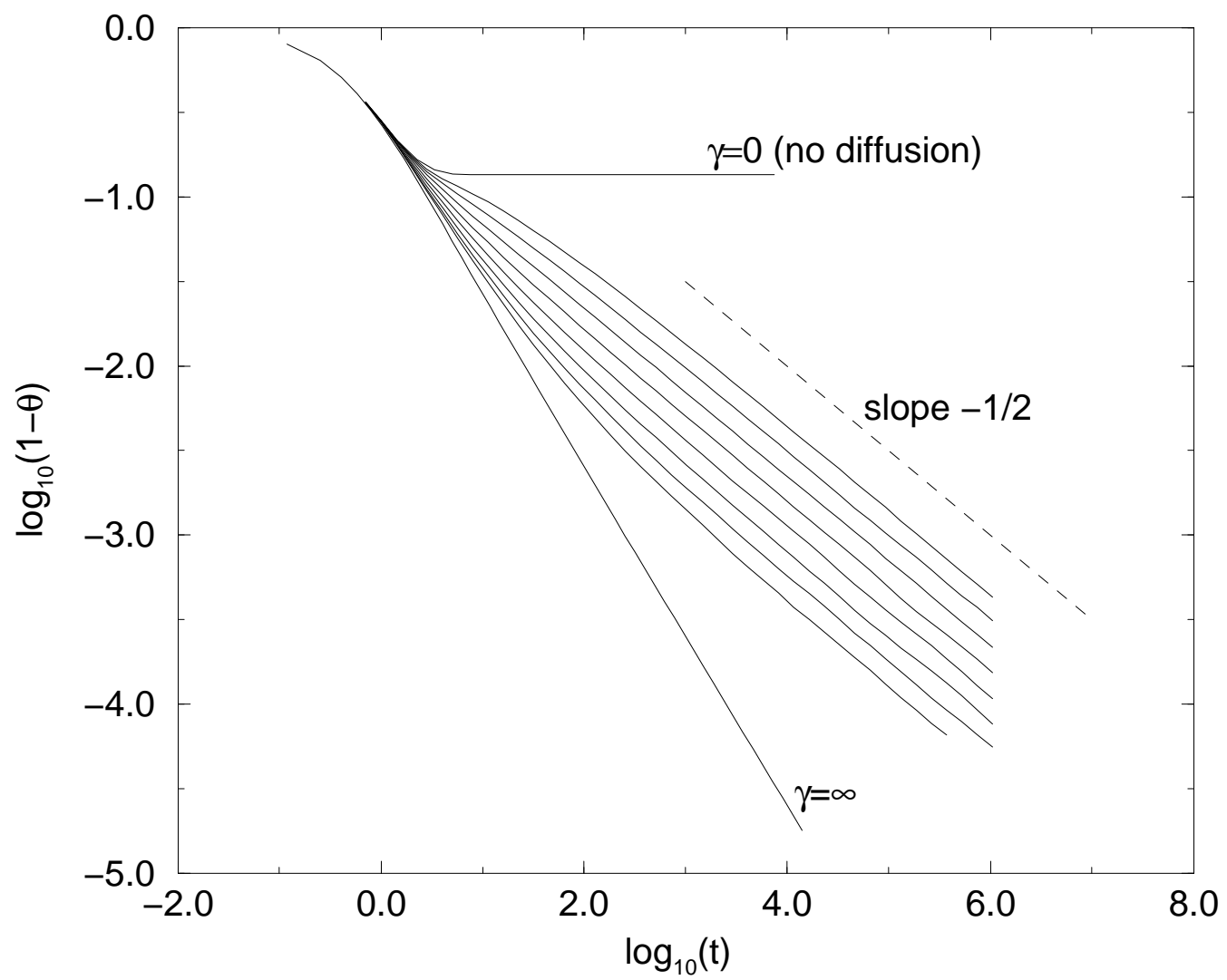


FIG.13.

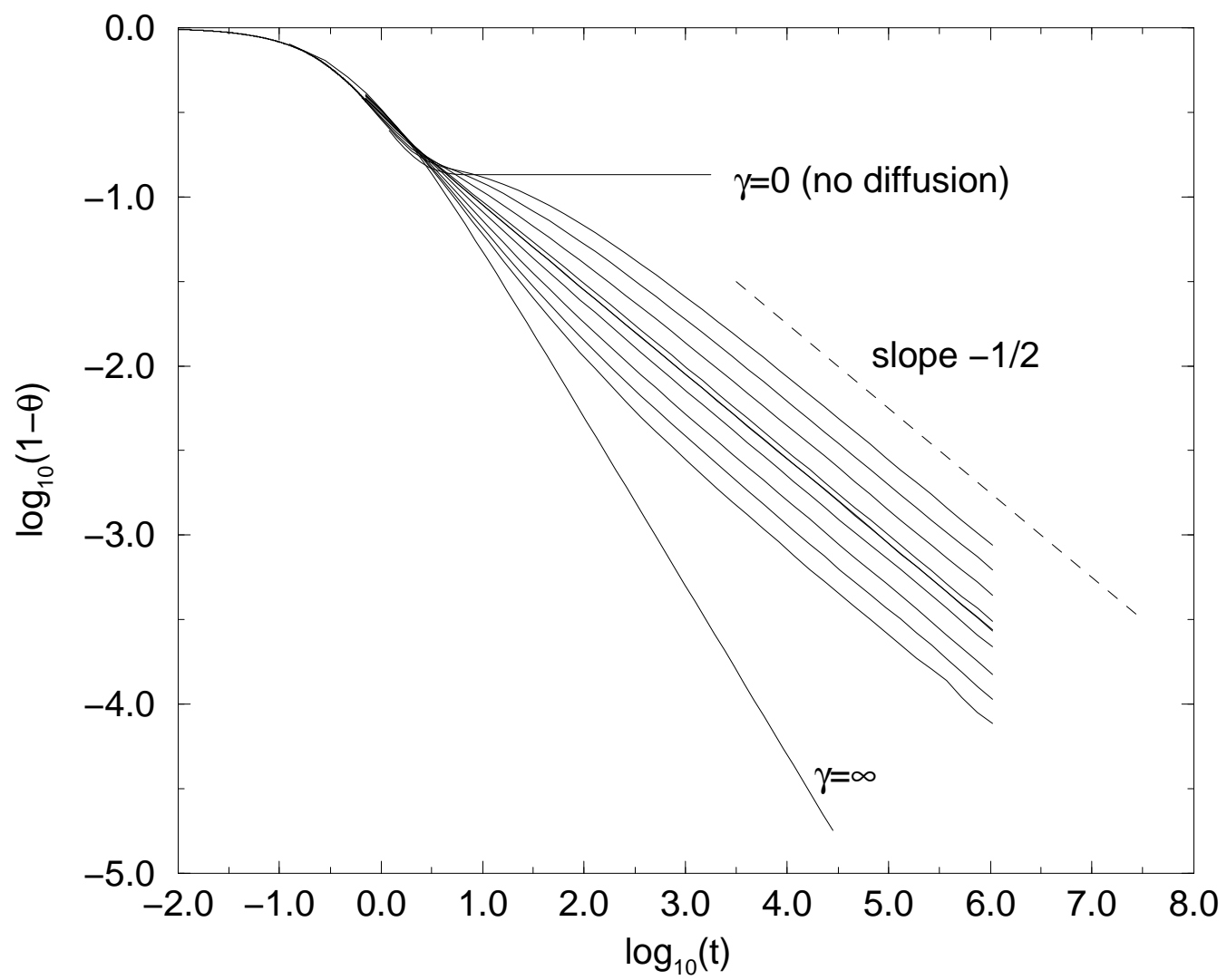


FIG.14.

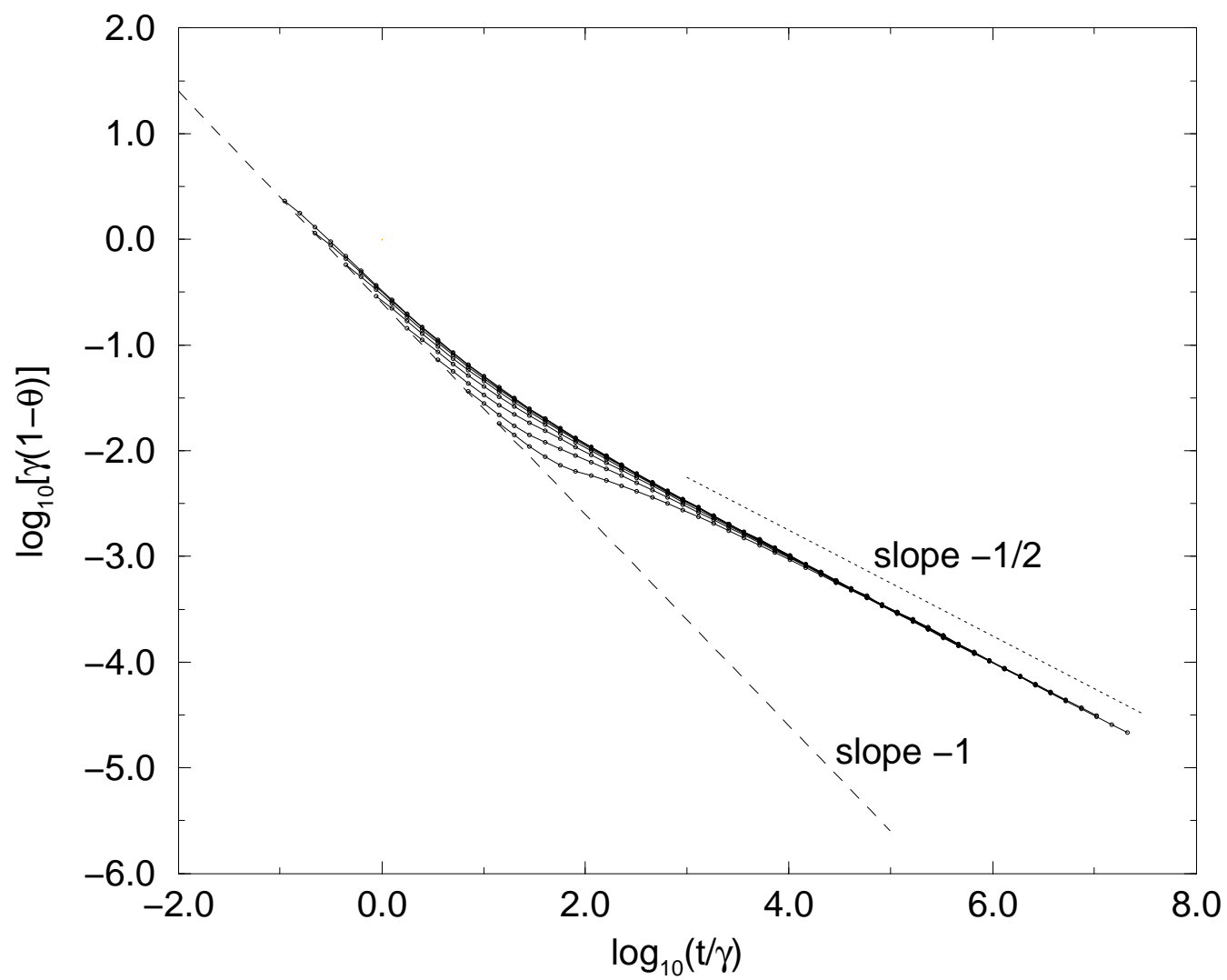


FIG.15.

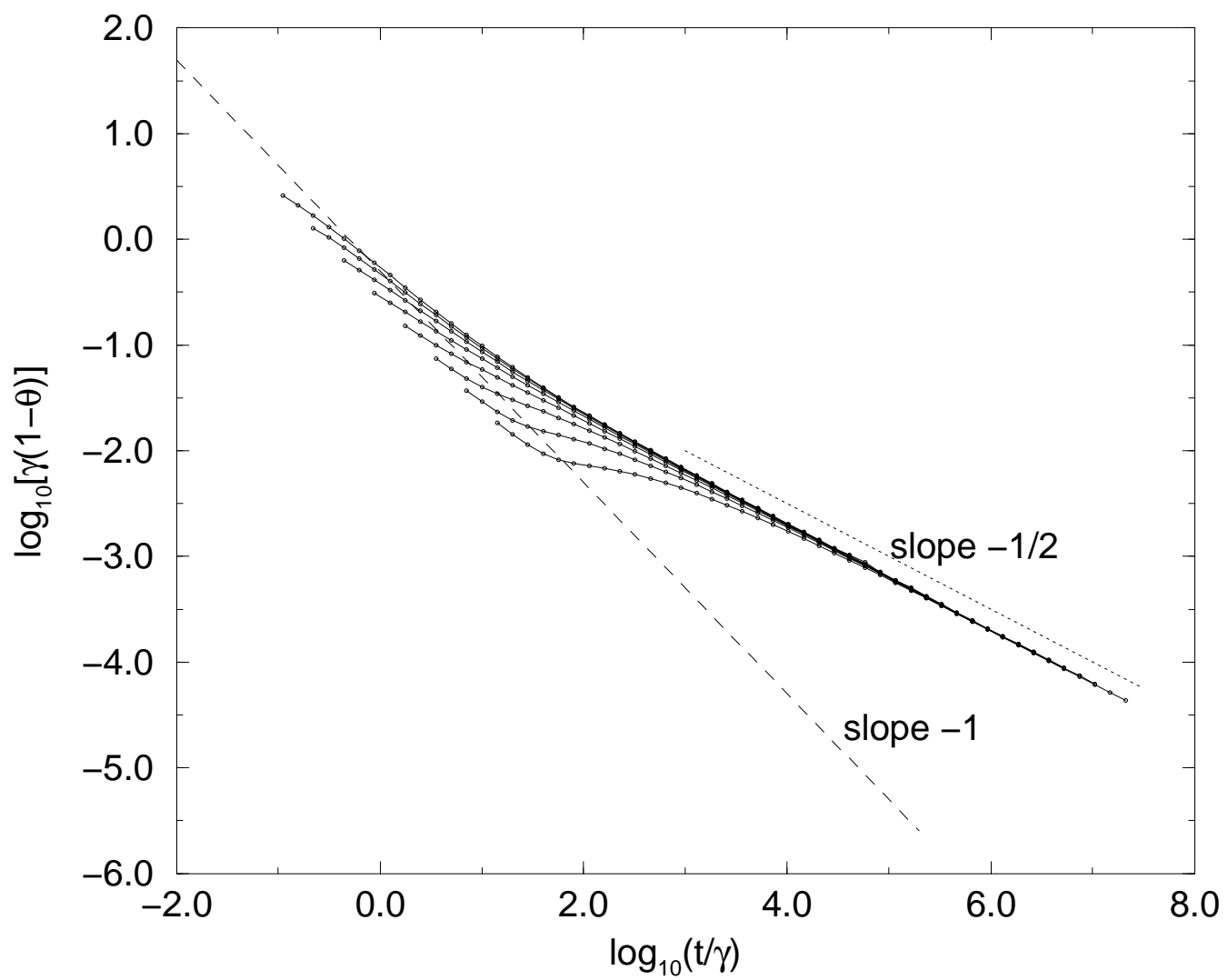


FIG.16.

APPENDIX A: THE SERIES EXPANSION COEFFICIENTS FOR DIFFUSIVE DIMER AND MONOMER MODELS

For the diffusive dimer model, the series expansion coefficients $P(\circ)^{(n)}$ for $n = 0, 1, 2, \dots, 31$ are

$$P(\circ)^{(0)} = 1,$$

$$P(\circ)^{(1)} = -2,$$

$$P(\circ)^{(2)} = 6,$$

$$P(\circ)^{(3)} = -22,$$

$$P(\circ)^{(4)} = 94,$$

$$P(\circ)^{(5)} = -454 - 8\gamma,$$

$$P(\circ)^{(6)} = 2430 + 136\gamma + 32\gamma^2,$$

$$P(\circ)^{(7)} = -14214 - 1648\gamma - 544\gamma^2 - 160\gamma^3,$$

$$P(\circ)^{(8)} = 89918 + 17776\gamma + 6720\gamma^2 + 2752\gamma^3 + 896\gamma^4,$$

$$P(\circ)^{(9)} = -610182 - 183640\gamma - 75488\gamma^2 - 34848\gamma^3 - 15808\gamma^4 \\ - 5376\gamma^5,$$

$$P(\circ)^{(10)} = 4412798 + 1876824\gamma + 829504\gamma^2 + 406464\gamma^3 + 207840\gamma^4 \\ + 98560\gamma^5 + 33792\gamma^6,$$

$$P(\circ)^{(11)} = -33827974 - 19290560\gamma - 9193152\gamma^2 - 4688896\gamma^3 \\ - 2538496\gamma^4 - 1364672\gamma^5 - 651008\gamma^6 - 219648\gamma^7,$$

$$P(\circ)^{(12)} = 273646526 + 201202624\gamma + 104153760\gamma^2 + 55017632\gamma^3 \\ + 30829536\gamma^4 + 17641472\gamma^5 + 9613280\gamma^6 \\ + 4487168\gamma^7 + 1464320\gamma^8,$$

$$P(\circ)^{(13)} = -2326980998 - 2140434856\gamma - 1212903168\gamma^2 \\ - 664001632\gamma^3 - 381899008\gamma^4 - 226930976\gamma^5 \\ - 132747296\gamma^6 - 71354592\gamma^7 - 31943680\gamma^8 - 9957376\gamma^9,$$

$$P(\circ)^{(14)} = 20732504062 + 23292327080\gamma + 14540797344\gamma^2 \\ + 8274623072\gamma^3 + 4870602688\gamma^4 + 2973218272\gamma^5 \\ + 1818085760\gamma^6 + 1059060704\gamma^7 + 550524320\gamma^8 \\ + 233132032\gamma^9 + 68796416\gamma^{10},$$

$$P(\circ)^{(15)} = -192982729350 - 259697613072\gamma - 179401122720\gamma^2 \\ - 106542051936\gamma^3 - 64143045632\gamma^4 - 40012549568\gamma^5 \\ - 25252420800\gamma^6 - 15495356512\gamma^7 - 8810633856\gamma^8 \\ - 4369323616\gamma^9 - 1734705152\gamma^{10} - 481574912\gamma^{11},$$

$$\begin{aligned}
P(\circ)^{(16)} = & 1871953992254 + 2969098816016\gamma + 2275429063808\gamma^2 \\
& + 1416343409184\gamma^3 + 872645113632\gamma^4 + 554654077056\gamma^5 \\
& + 358789726592\gamma^6 + 228594111904\gamma^7 + 137952689120\gamma^8 \\
& + 75460620608\gamma^9 + 35391538304\gamma^{10} + 13105004544\gamma^{11} \\
& + 3408068608\gamma^{12},
\end{aligned}$$

$$\begin{aligned}
P(\circ)^{(17)} = & -18880288847750 - 34819585889272\gamma - 29629807780320\gamma^2 \\
& - 19414284425280\gamma^3 - 12257502997152\gamma^4 - 7925353240960\gamma^5 \\
& - 5232190291296\gamma^6 - 3433400249408\gamma^7 - 2164670388352\gamma^8 \\
& - 1265163225632\gamma^9 - 659040825216\gamma^{10} - 290843555840\gamma^{11} \\
& - 100193632256\gamma^{12} - 24343347200\gamma^{13},
\end{aligned}$$

$$\begin{aligned}
P(\circ)^{(18)} = & 197601208474238 + 418857922740216\gamma + 395602299173696\gamma^2 \\
& + 273978158172160\gamma^3 + 177588283397088\gamma^4 \\
& + 116718001713792\gamma^5 + 78414883481952\gamma^6 \\
& + 52726551390048\gamma^7 + 34420850096512\gamma^8 + 21138424854304\gamma^9 \\
& + 11830865489344\gamma^{10} + 5828807502880\gamma^{11} + 2414315305984\gamma^{12} \\
& + 773310775296\gamma^{13} + 175272099840\gamma^{14},
\end{aligned}$$

$$\begin{aligned}
P(\circ)^{(19)} = & -2142184050841734 - 5167334116337248\gamma \\
& - 5409353469693312\gamma^2 - 3974358277418464\gamma^3 \\
& - 2650710992073376\gamma^4 - 1770760359697088\gamma^5 \\
& - 1208250123782816\gamma^6 - 829498459619104\gamma^7 \\
& - 557514170611008\gamma^8 - 356342440781248\gamma^9 \\
& - 210643968436256\gamma^{10} - 111995901788096\gamma^{11} \\
& - 51951090626080\gamma^{12} - 20179683365760\gamma^{13} \\
& - 6013648437248\gamma^{14} - 1270722723840\gamma^{15},
\end{aligned}$$

$$\begin{aligned}
P(\circ)^{(20)} = & 24016181943732414 + 65354875319253600\gamma + 75674015695071776\gamma^2 \\
& + 59170426635099072\gamma^3 + 40709461342679712\gamma^4 \\
& + 27654553375343168\gamma^5 + 19139165182573632\gamma^6 \\
& + 13379477948777856\gamma^7 + 9220546462388512\gamma^8 \\
& + 6096023066059456\gamma^9 + 3768570926043360\gamma^{10} \\
& + 2126161230748448\gamma^{11} + 1067953378669088\gamma^{12} \\
& + 465021052820384\gamma^{13} + 169438907614560\gamma^{14} \\
& + 47047244775424\gamma^{15} + 9268801044480\gamma^{16},
\end{aligned}$$

$$\begin{aligned}
P(\circ)^{(21)} = & -278028611833689478 - 847070521919796296\gamma \\
& - 1082140708741735168\gamma^2 - 902807166330596704\gamma^3 \\
& - 642463112877878368\gamma^4 - 444202148035295936\gamma^5 \\
& - 311557082954071776\gamma^6 - 221310190035972736\gamma^7 \\
& - 155891975926137920\gamma^8 - 106130622734975296\gamma^9 \\
& - 68163212990088160\gamma^{10} - 40401083210384096\gamma^{11} \\
& - 21628549879148512\gamma^{12} - 10224685696979776\gamma^{13} \\
& - 4170519535181536\gamma^{14} - 1426800665301088\gamma^{15} \\
& - 369849931661312\gamma^{16} - 67971207659520\gamma^{17},
\end{aligned}$$

$$\begin{aligned}
P(\circ)^{(22)} = & 3319156078802044158 + 11245724095683198280\gamma \\
& + 15806297066594859744\gamma^2 + 14097805354882121664\gamma^3 \\
& + 10405357836443942528\gamma^4 + 7331412297306645056\gamma^5 \\
& + 5209126487226619872\gamma^6 + 3753693513361866688\gamma^7 \\
& + 2695682775965810496\gamma^8 + 1883121553855520800\gamma^9 \\
& + 1250352187435821024\gamma^{10} + 773119232263912256\gamma^{11} \\
& + 436759047669796704\gamma^{12} + 221031829068739616\gamma^{13} \\
& + 98090146080366016\gamma^{14} + 37415367315785664\gamma^{15} \\
& + 12034887222344992\gamma^{16} + 2918797259309056\gamma^{17} \\
& + 500840477491200\gamma^{18},
\end{aligned}$$

$$\begin{aligned}
P(\circ)^{(23)} = & -40811417293301014150 - 152849819143271186864\gamma \\
& - 235669362697015641504\gamma^2 - 225030434256866474048\gamma^3 \\
& - 172730720539355533536\gamma^4 - 124209020387171547840\gamma^5 \\
& - 89396791275859021472\gamma^6 - 65265468008645791072\gamma^7 \\
& - 47681226234984815648\gamma^8 - 34078914479620848544\gamma^9 \\
& - 23302022034195791264\gamma^{10} - 14950154580712363008\gamma^{11} \\
& - 8846189597178252768\gamma^{12} - 4745848875738292928\gamma^{13} \\
& - 2265231509811056512\gamma^{14} - 941951799608143040\gamma^{15} \\
& - 335416253872860704\gamma^{16} - 101595547064760928\gamma^{17} \\
& - 23107112699691008\gamma^{18} - 3706219533434880\gamma^{19},
\end{aligned}$$

$$\begin{aligned}
P(\circ)^{(24)} = & 516247012345341914942 + 2125833345702860926128\gamma \\
& + 3584709736316916197120\gamma^2 + 3667635825937886265248\gamma^3 \\
& + 2935302250997270008320\gamma^4 + 2157911658548001672192\gamma^5 \\
& + 1573612047377468555296\gamma^6 + 1162780482970536810112\gamma^7 \\
& + 862635165194788176384\gamma^8 + 629254138123646209984\gamma^9 \\
& + 441670494784119415040\gamma^{10} + 292773697423309629888\gamma^{11} \\
& + 180386574048628422176\gamma^{12} + 101774434388607688384\gamma^{13} \\
& + 51747976608776753696\gamma^{14} + 23266775394437326144\gamma^{15} \\
& + 9052145344807326144\gamma^{16} + 3002516812188788608\gamma^{17} \\
& + 857815531941631296\gamma^{18} + 183397309348839424\gamma^{19} \\
& + 27531916534087680\gamma^{20},
\end{aligned}$$

$$\begin{aligned}
P(\circ)^{(25)} = & -6711185258405244576646 - 30238180002704596333208\gamma \\
& - 55598200570861707979680\gamma^2 - 60976389483506749681568\gamma^3 \\
& - 51003312645322864268128\gamma^4 - 38404740494773062950176\gamma^5 \\
& - 28389964187770573475040\gamma^6 - 21217507587703139716128\gamma^7 \\
& - 15959639632228805304256\gamma^8 - 11856781604498555126144\gamma^9 \\
& - 8519923504665486348256\gamma^{10} - 5814814052946982013216\gamma^{11} \\
& - 3713060409585399321472\gamma^{12} - 2188983105017137174464\gamma^{13} \\
& - 1175478617129581490560\gamma^{14} - 566022591719541854336\gamma^{15} \\
& - 239600608251046218528\gamma^{16} - 87093953947019843424\gamma^{17} \\
& - 26826301792524728832\gamma^{18} - 7241192306564087872\gamma^{19} \\
& - 1458610850414723072\gamma^{20} - 205237923254108160\gamma^{21},
\end{aligned}$$

$$\begin{aligned}
P(\circ)^{(26)} = & 89574471680939133937534 + 439663978304010761309336\gamma \\
& + 878864969592056661663680\gamma^2 + 1033220218894344066221152\gamma^3 \\
& + 905162593426518959688480\gamma^4 + 699466982856423681626592\gamma^5 \\
& + 524550622363351486026048\gamma^6 + 396321792642538988104928\gamma^7 \\
& + 301868194425498598076992\gamma^8 + 227989242191471816249696\gamma^9 \\
& + 167333371520455599867424\gamma^{10} + 117243269450611152416000\gamma^{11} \\
& + 77295857780714519060928\gamma^{12} + 47370056124944928474784\gamma^{13} \\
& + 26675453205517382525856\gamma^{14} + 13627834185309074754720\gamma^{15} \\
& + 6215448113411854023776\gamma^{16} + 2476949102568415569728\gamma^{17} \\
& + 839899058850812411936\gamma^{18} + 239165277641087918144\gamma^{19} \\
& + 61092781558844261824\gamma^{20} + 11620352278518562816\gamma^{21} \\
& + 1534822730422026240\gamma^{22},
\end{aligned}$$

$$\begin{aligned}
P(\circ)^{(27)} = & -1226366187219563392423046 - 6531379936679608555490048\gamma \\
& - 14153158560229748831123712\gamma^2 - 17829942516341618875683488\gamma^3 \\
& - 16390388657713777384337248\gamma^4 - 13024188161033852626760832\gamma^5 \\
& - 9918027745419496427963072\gamma^6 - 7573935646469621224533504\gamma^7 \\
& - 5835396744531198025370240\gamma^8 - 4473355152862831429807584\gamma^9 \\
& - 3346869880800982736546432\gamma^{10} - 2401496033284393106394304\gamma^{11} \\
& - 1629516516241948614285760\gamma^{12} - 1033801940311680754546112\gamma^{13} \\
& - 607038025256747982659264\gamma^{14} - 326452128844455325407648\gamma^{15} \\
& - 158757402409409198571968\gamma^{16} - 68639251401951128448448\gamma^{17} \\
& - 25759744940242270466976\gamma^{18} - 8133338764734443700064\gamma^{19} \\
& - 2127377128471631380160\gamma^{20} - 515040012051367812096\gamma^{21} \\
& - 92704039977088974848\gamma^{22} - 11511170478165196800\gamma^{23},
\end{aligned}$$

$$\begin{aligned}
P(\circ)^{(28)} = & 17208434165059531880467902 + 99081506420313710986772736\gamma \\
& + 232103903429219081532907872\gamma^2 + 313143052910337271943545632\gamma^3 \\
& + 302531882137452591255077248\gamma^4 + 247695203872064524469329920\gamma^5 \\
& + 191751044433982602086189184\gamma^6 + 148003121016823516846598336\gamma^7 \\
& + 115246426164717743454533376\gamma^8 + 89548623260586320065607520\gamma^9 \\
& + 68178700940595222195124032\gamma^{10} + 49993383490006417316624128\gamma^{11} \\
& + 34821933734970293328723264\gamma^{12} + 22791830094404699697241952\gamma^{13} \\
& + 13891323265031765512465344\gamma^{14} + 7814665824226532852984960\gamma^{15} \\
& + 4016982900101880080201440\gamma^{16} + 1862205866467120855344800\gamma^{17} \\
& + 764317776739694865201344\gamma^{18} + 270291929328683129059200\gamma^{19} \\
& + 79296629516951459720032\gamma^{20} + 18879546837921695785504\gamma^{21} \\
& + 4338110967536077063424\gamma^{22} + 740404461632374177792\gamma^{23} \\
& + 86564001995802279936\gamma^{24},
\end{aligned}$$

$$\begin{aligned}
P(\circ)^{(29)} = & -247289888972538586949878150 - 1534172692240041452626636520\gamma \\
& - 3874787071735125029536527360\gamma^2 - 5593914936389904746992944000\gamma^3 \\
& - 5687097195642308827551818432\gamma^4 - 4806905879064545608139517504\gamma^5 \\
& - 3787785163974288880030601664\gamma^6 - 2955603108243908695631102784\gamma^7 \\
& - 2324464815975057231796395232\gamma^8 - 1828539431234039817220631104\gamma^9 \\
& - 1414541083036286620968100704\gamma^{10} - 1058040639042272841296197632\gamma^{11}
\end{aligned}$$

$$\begin{aligned}
& -754795598374307863822508064\gamma^{12} - 508234645790343970597871232\gamma^{13} \\
& -320323245811479831435568800\gamma^{14} - 187552827879867728682574240\gamma^{15} \\
& -101194015894779754258916928\gamma^{16} - 49808752256243832593146240\gamma^{17} \\
& -22057128789803220776595968\gamma^{18} - 8610553430581355224855168\gamma^{19} \\
& -2871992002592102396999904\gamma^{20} - 781079045618282247374272\gamma^{21} \\
& -167173262847020276611008\gamma^{22} - 36502951600975155899648\gamma^{23} \\
& -5918914576756420640768\gamma^{24} - 652559399660663341056\gamma^{25},
\end{aligned}$$

$$\begin{aligned}
P(\circ)^{(30)} = & 3636599975026505414628377086 + 24235192834488592555063381480\gamma \\
& + 65825866944987465106280540640\gamma^2 + 101588178322920631379346693376\gamma^3 \\
& + 108792583977960919823164346304\gamma^4 + 95106347438122321463161286528\gamma^5 \\
& + 76389237086435129240476170944\gamma^6 + 60282902962582074896568152544\gamma^7 \\
& + 47861156428195317146948964544\gamma^8 + 38077374671506940952543821152\gamma^9 \\
& + 29889064803981070602563425824\gamma^{10} + 22767753081638239927853052832\gamma^{11} \\
& + 16603099771615247450036647104\gamma^{12} + 11473120418073147648994092160\gamma^{13} \\
& + 7454372028423481067708753792\gamma^{14} + 4523940784361767910490004224\gamma^{15} \\
& + 2547674890838510347194642304\gamma^{16} + 1321026477071424198196864544\gamma^{17} \\
& + 624158962537014248104138272\gamma^{18} + 264717889700048519760895712\gamma^{19} \\
& + 98517274209783711927693664\gamma^{20} + 31032886905928789132563200\gamma^{21} \\
& + 7806681142471034370768032\gamma^{22} + 1477165355656235095757792\gamma^{23} \\
& + 306829936381452586376960\gamma^{24} + 47352796340581207900160\gamma^{25} \\
& + 4930448797436123021312\gamma^{26},
\end{aligned}$$

$$\begin{aligned}
P(\circ)^{(31)} = & -54690132113431117456486546054 - 390402306358974047554407998032\gamma \\
& -1137582424553489289447807997792\gamma^2 - 1874665509618062031115241291296\gamma^3 \\
& -2116316617323806096783903601344\gamma^4 - 1916826452624015867653776105344\gamma^5 \\
& -1571619063016185146258668134144\gamma^6 - 1255045527053951534543760304384\gamma^7 \\
& -1005606717413244521960545134816\gamma^8 - 808411234967533218962071194176\gamma^9 \\
& -643116053649141335307306261344\gamma^{10} - 498189822261377252029700331328\gamma^{11} \\
& -370737701124192040949130562656\gamma^{12} - 262369454324949422539656437184\gamma^{13} \\
& -175268684516776147755547530080\gamma^{14} - 109871960830604539165436865664\gamma^{15} \\
& -64284643706828638935486335392\gamma^{16} - 34893515783410832792353344544\gamma^{17} \\
& -17434380523486099607832839808\gamma^{18} - 7930481323762069309980955744\gamma^{19} \\
& -3230836698378503824136216160\gamma^{20} - 1149328018944519338194160160\gamma^{21} \\
& -342504050878779281408793504\gamma^{22} - 79568648016407862847405792\gamma^{23} \\
& -13027718319821439160157152\gamma^{24} - 2576298242354693706469632\gamma^{25} \\
& -379070964781663249235968\gamma^{26} - 37330540894873502875648\gamma^{27}.
\end{aligned}$$

For the diffusive monomer model, we have

$$P(\circ)^{(0)} = 1,$$

$$P(\circ)^{(1)} = -2,$$

$$P(\circ)^{(2)} = 6,$$

$$P(\circ)^{(3)} = -22 + 4\gamma,$$

$$\begin{aligned}
P(\circ)^{(4)} &= 94 - 40\gamma - 16\gamma^2, \\
P(\circ)^{(5)} &= -454 + 316\gamma + 136\gamma^2 + 80\gamma^3, \\
P(\circ)^{(6)} &= 2430 - 2384\gamma - 840\gamma^2 - 608\gamma^3 - 448\gamma^4, \\
P(\circ)^{(7)} &= -14214 + 18116\gamma + 4240\gamma^2 + 3072\gamma^3 + 3136\gamma^4 + 2688\gamma^5, \\
P(\circ)^{(8)} &= 89918 - 141432\gamma - 13920\gamma^2 - 9728\gamma^3 - 13120\gamma^4 - 17664\gamma^5 - 16896\gamma^6, \\
P(\circ)^{(9)} &= -610182 + 1143564\gamma - 52040\gamma^2 - 21072\gamma^3 + 16416\gamma^4 + 60480\gamma^5 \\
&\quad + 105600\gamma^6 + 109824\gamma^7, \\
P(\circ)^{(10)} &= 4412798 - 9606304\gamma + 1860776\gamma^2 + 776864\gamma^3 \\
&\quad + 366240\gamma^4 + 76544\gamma^5 - 285824\gamma^6 - 658944\gamma^7 - 732160\gamma^8, \\
P(\circ)^{(11)} &= -33827974 + 83906644\gamma - 28877184\gamma^2 - 9589600\gamma^3 \\
&\quad - 5139808\gamma^4 - 3368896\gamma^5 - 1464064\gamma^6 \\
&\quad + 1317888\gamma^7 + 4246528\gamma^8 + 4978688\gamma^9, \\
P(\circ)^{(12)} &= 273646526 - 761825992\gamma + 377695696\gamma^2 + 89195520\gamma^3 \\
&\quad + 45390432\gamma^4 + 35391872\gamma^5 + 28371968\gamma^6 \\
&\quad + 15465472\gamma^7 - 5471232\gamma^8 - 28061696\gamma^9 - 34398208\gamma^{10}, \\
P(\circ)^{(13)} &= -2326980998 + 7184044444\gamma - 4654680536\gamma^2 \\
&\quad - 637249840\gamma^3 - 288190208\gamma^4 - 259172928\gamma^5 \\
&\quad - 257515008\gamma^6 - 227319040\gamma^7 - 137749504\gamma^8 \\
&\quad + 15841280\gamma^9 + 189190144\gamma^{10} + 240787456\gamma^{11}, \\
P(\circ)^{(14)} &= 20732504062 - 70283711216\gamma + 56240459224\gamma^2 \\
&\quad + 2043271904\gamma^3 + 731559936\gamma^4 + 1283891648\gamma^5 \\
&\quad + 1667097280\gamma^6 + 1836321792\gamma^7 + 1684263680\gamma^8 \\
&\quad + 1097334784\gamma^9 + 33075200\gamma^{10} - 1296547840\gamma^{11} \\
&\quad - 1704034304\gamma^{12}, \\
P(\circ)^{(15)} &= -192982729350 + 712495690468\gamma - 678540577872\gamma^2 \\
&\quad + 43943729216\gamma^3 + 15689764160\gamma^4 - 248456832\gamma^5 \\
&\quad - 6690721088\gamma^6 - 9906840832\gamma^7 - 11246331136\gamma^8 \\
&\quad - 10574563328\gamma^9 - 7651909632\gamma^{10} - 1206583296\gamma^{11} \\
&\quad + 9007038464\gamma^{12} + 12171673600\gamma^{13}, \\
P(\circ)^{(16)} &= 1871953992254 - 7474944990488\gamma + 8253899207808\gamma^2 \\
&\quad - 1370040257024\gamma^3 - 372411184768\gamma^4 \\
&\quad - 94316090496\gamma^5 - 14702702272\gamma^6 + 15363239488\gamma^7 \\
&\quad + 29522467968\gamma^8 + 35529220864\gamma^9 + 38287712768\gamma^{10} \\
&\quad + 40591720448\gamma^{11} + 15336308736\gamma^{12} - 63292702720\gamma^{13} \\
&\quad - 87636049920\gamma^{14},
\end{aligned}$$

$$\begin{aligned}
P(\circ)^{(17)} = & -18880288847750 + 81057814178860\gamma - 101782506154664\gamma^2 \\
& + 27189637704816\gamma^3 + 5335958139680\gamma^4 + 1434188162432\gamma^5 \\
& + 658007059712\gamma^6 + 490637978560\gamma^7 + 478988103296\gamma^8 \\
& + 504910140800\gamma^9 + 504004959232\gamma^{10} + 347157901824\gamma^{11} \\
& - 27525865472\gamma^{12} - 157623173120\gamma^{13} + 449134755840\gamma^{14} \\
& + 635361361920\gamma^{15},
\end{aligned}$$

$$\begin{aligned}
P(\circ)^{(18)} = & 197601208474238 - 907450604595520\gamma \\
& + 1276490317628872\gamma^2 - 469854934268320\gamma^3 \\
& - 57231645622432\gamma^4 - 12599010163904\gamma^5 - 8136201575040\gamma^6 \\
& - 8857562356800\gamma^7 - 10650704276864\gamma^8 - 12583232475008\gamma^9 \\
& - 14215451977344\gamma^{10} - 14614504454144\gamma^{11} \\
& - 11416776989184\gamma^{12} - 3717889196032\gamma^{13} + 1478858342400\gamma^{14} \\
& - 3214181007360\gamma^{15} - 4634400522240\gamma^{16},
\end{aligned}$$

$$\begin{aligned}
P(\circ)^{(19)} = & -2142184050841734 + 10475986286134644\gamma \\
& - 16312769443915296\gamma^2 + 7646757249760992\gamma^3 \\
& + 364024229452512\gamma^4 + 20915048148288\gamma^5 \\
& + 60965998050816\gamma^6 + 104195753619392\gamma^7 + 143529329474688\gamma^8 \\
& + 180347215997184\gamma^9 + 214040019465728\gamma^{10} \\
& + 242779230361408\gamma^{11} + 251416724734720\gamma^{12} \\
& + 201407890808064\gamma^{13} + 80080105439232\gamma^{14} \\
& - 13205549875200\gamma^{15} + 23172002611200\gamma^{16} \\
& + 33985603829760\gamma^{17},
\end{aligned}$$

$$\begin{aligned}
P(\circ)^{(20)} = & 24016181943732414 - 124577072070506344\gamma \\
& + 212664085816703088\gamma^2 - 121030264397636800\gamma^3 \\
& + 3207001016515744\gamma^4 + 1926788775361664\gamma^5 \\
& - 97846534908224\gamma^6 - 1011525246587968\gamma^7 \\
& - 1613872175868224\gamma^8 - 2122232829566464\gamma^9 \\
& - 2582498914206400\gamma^{10} - 3029609305192704\gamma^{11} \\
& - 3468160142157312\gamma^{12} - 3654216100258816\gamma^{13} \\
& - 2984599157455872\gamma^{14} - 1274373807013888\gamma^{15} \\
& + 114396518154240\gamma^{16} - 168139303157760\gamma^{17} \\
& - 250420238745600\gamma^{18},
\end{aligned}$$

$$\begin{aligned}
P(\circ)^{(21)} = & -278028611833689478 + 1524422965551679164\gamma \\
& - 2830011720336190520\gamma^2 + 1893620809129623184\gamma^3 \\
& - 190312900454425856\gamma^4 - 52429573013981632\gamma^5 \\
& - 5696486069346432\gamma^6 + 8870271163894976\gamma^7 \\
& + 16508258449035520\gamma^8 + 22318365235658944\gamma^9 \\
& + 27330506775020352\gamma^{10} + 32127595322607680\gamma^{11} \\
& + 37750764697213632\gamma^{12} + 44585314916972224\gamma^{13} \\
& + 48710458796935168\gamma^{14} + 40826850701992704\gamma^{15} \\
& + 18137503276204032\gamma^{16} - 971272783134720\gamma^{17} \\
& + 1227059169853440\gamma^{18} + 1853109766717440\gamma^{19},
\end{aligned}$$

$$\begin{aligned}
P(\circ)^{(22)} = & 3319156078802044158 - 19176747359879923600\gamma \\
& + 38453690823403414456\gamma^2 - 29561658453026305696\gamma^3 \\
& + 5155032487045587520\gamma^4 + 942243974334873216\gamma^5 \\
& + 105439299259768768\gamma^6 - 81111203950262400\gamma^7 \\
& - 160997366287047168\gamma^8 - 215954557589465664\gamma^9 \\
& - 259399767952654784\gamma^{10} - 296956113372155968\gamma^{11} \\
& - 341510419736224256\gamma^{12} - 415727829470043072\gamma^{13} \\
& - 528023625074855232\gamma^{14} - 615174223548672512\gamma^{15} \\
& - 534970609920598272\gamma^{16} - 244776032213663744\gamma^{17} \\
& + 8131502895267840\gamma^{18} - 9000818866913280\gamma^{19} \\
& - 13765958267043840\gamma^{20},
\end{aligned}$$

$$\begin{aligned}
P(\circ)^{(23)} = & -40811417293301014150 + 247769892998148929540\gamma \\
& - 533551218840123871408\gamma^2 + 463133218427313661568\gamma^3 \\
& - 114908031635611603008\gamma^4 - 13026651600988443520\gamma^5 \\
& - 694835794636118976\gamma^6 + 985945653624581504\gamma^7 \\
& + 1559657950629139840\gamma^8 + 1927443716610738944\gamma^9 \\
& + 2162116688501650432\gamma^{10} + 2286453247614987008\gamma^{11} \\
& + 2406004053525926464\gamma^{12} + 2793344171831971456\gamma^{13} \\
& + 3867839365244115904\gamma^{14} + 5768757000308409472\gamma^{15} \\
& + 7479458725939469568\gamma^{16} + 6842447109112948224\gamma^{17} \\
& + 3214950387582763008\gamma^{18} - 67385809698816000\gamma^{19} \\
& + 66326889832120320\gamma^{20} + 102618961627054080\gamma^{21},
\end{aligned}$$

$$\begin{aligned}
P(\circ)^{(24)} = & 516247012345341914942 - 3285119025877372180920\gamma \\
& + 7559108520607773843488\gamma^2 - 7308871611544450832064\gamma^3 \\
& + 2350981727669407843776\gamma^4 + 118905993297229011008\gamma^5 \\
& - 16790780767539633792\gamma^6 - 16613440672679879680\gamma^7 \\
& - 15548046461070182784\gamma^8 - 15384986519988719936\gamma^9 \\
& - 14161472648995235136\gamma^{10} - 11276361716222164096\gamma^{11} \\
& - 7324030172672791168\gamma^{12} - 4587460726218948608\gamma^{13} \\
& - 8052405463773808896\gamma^{14} - 24820684069180820672\gamma^{15} \\
& - 56960923428566366080\gamma^{16} - 88298755351002966272\gamma^{17} \\
& - 86378467061276064256\gamma^{18} - 41668128760418795520\gamma^{19} \\
& + 554175039327436800\gamma^{20} - 490786338216345600\gamma^{21} \\
& - 767411365211013120\gamma^{22},
\end{aligned}$$

$$\begin{aligned}
P(\circ)^{(25)} = & -6711185258405244576646 + 44661059313146988290380\gamma \\
& - 109331606843615382157384\gamma^2 + 116480278944698068262320\gamma^3 \\
& - 46011745270359552516256\gamma^4 + 440850798604678021632\gamma^5 \\
& + 792105834451739504064\gamma^6 + 305738012971578476416\gamma^7 \\
& + 159590366941358300288\gamma^8 + 95740210483655793728\gamma^9 \\
& + 30567600232164220480\gamma^{10} - 56955396275740956800\gamma^{11} \\
& - 166253571659143480512\gamma^{12} - 281518130521880300608\gamma^{13} \\
& - 362613423701499252928\gamma^{14} - 326561982884636510016\gamma^{15} \\
& - 57663159522038980416\gamma^{16} + 474502223919197873792\gamma^{17}
\end{aligned}$$

$$\begin{aligned}
& +1016510392155756708096\gamma^{18} + 1083954865492145854976\gamma^{19} \\
& +537244083313897897984\gamma^{20} - 4530850240533626880\gamma^{21} \\
& +3645203984752312320\gamma^{22} + 5755585239082598400\gamma^{23},
\end{aligned}$$

$$\begin{aligned}
P(\circ)^{(26)} = & 89574471680939133937534 - 622083509256483761778144\gamma \\
& +1613972832019449938327400\gamma^2 - 1877838552918714034411104\gamma^3 \\
& +879136906924104701402400\gamma^4 - 60203145083669334396480\gamma^5 \\
& -20498110028978700736576\gamma^6 - 5129659282973757956032\gamma^7 \\
& -1545427282000245352192\gamma^8 - 81470942122801407680\gamma^9 \\
& +1260555105289740810752\gamma^{10} + 2895967959719246612096\gamma^{11} \\
& +4862870780663281576640\gamma^{12} + 7053872326919183964416\gamma^{13} \\
& +9217493906833607526464\gamma^{14} + 10750408710797132958720\gamma^{15} \\
& +10329246189184106668160\gamma^{16} + 6079839402236030452352\gamma^{17} \\
& -2473100644141600758272\gamma^{18} - 11423977927106528212480\gamma^{19} \\
& -13587010293017989388288\gamma^{20} - 6925115206590254809088\gamma^{21} \\
& +36874116098389180416\gamma^{22} - 27166362328469864448\gamma^{23} \\
& -43282000997901139968\gamma^{24},
\end{aligned}$$

$$\begin{aligned}
P(\circ)^{(27)} = & -1226366187219563392423046 + 8871463075992006738446996\gamma \\
& -24310664899996326040840960\gamma^2 + 30660793724129104401682976\gamma^3 \\
& -16590293346041070916979232\gamma^4 + 2101735937627830336699008\gamma^5 \\
& +414485759213945048620480\gamma^6 + 69997075687476971109760\gamma^7 \\
& +9796719680443211190976\gamma^8 - 12989214479805658674880\gamma^9 \\
& -34255224236967502762880\gamma^{10} - 59677881433243896747264\gamma^{11} \\
& -89567316898510113800576\gamma^{12} - 122844647469002814372800\gamma^{13} \\
& -158096743387017593763520\gamma^{14} - 192783430108635063948928\gamma^{15} \\
& -218698994059862664719168\gamma^{16} - 214808919929359674024448\gamma^{17} \\
& -150396704456781735005888\gamma^{18} - 17357306803247632596736\gamma^{19} \\
& +125070331075601599340800\gamma^{20} + 170681832575907668260864\gamma^{21} \\
& +89515662319906963062784\gamma^{22} - 299007080543601819648\gamma^{23} \\
& +203092466220920733696\gamma^{24} + 326279699830331670528\gamma^{25}.
\end{aligned}$$